

Studies on scale-up theory for lyophilization process

- Equivalent resistance model and process analytical technology -

2019, March

Hidenori Kawasaki

Table of contents

Chapter 1	General Introduction	4
Chapter 2	Scale-Up Procedure for Primary Drying Process in Lyophilizer by Using the Vial Heat Transfer and the Drying Resistance	8
2.1	Introduction	8
2.2	Experimental	12
2.2.1	Materials	12
2.2.2	Physical Property Evaluation of Flomoxef Sodium Bulk Solution	13
2.2.3	Estimate of Vial Heat Transfer Coefficient	13
2.2.4	Evaluation of the Water Vapor Transfer Resistance of the Dried Layer	14
2.2.5	Verification Study in the Production Lyophilizer	15
2.3	Result and Discussion	16
2.3.1	Physical Property Evaluation of Flomoxef Sodium Bulk Solution	16
2.3.2	Comparison of Sublimation Behavior in Both Machines	17
2.3.3	Contribution of Elemental Process of Heat Transfer to Vial Heat Transfer	21
2.3.4	Monitoring of Temperature Profile for Design of Operation Conditions	23
2.3.5	Scale-Up of Pilot to Production Lyophilizer	24
2.4	Conclusion	26
2.5	Appendix A Elucidation of K_v Based on the Heat/Mass Transfer	27
2.6	Appendix B Decomposition of K_v into Elemental Factors	28
2.7	Appendix C Prediction of T_b and T_{ice} for Verification Test	30
Chapter 3:	Effect of Controlled Nucleation of Ice Crystals on the Primary Drying Stage during Lyophilization	34
3.1	Introduction	34
3.2	Experimental	36
3.3.1	Materials	36
3.3.2	Analytical Procedure	37
3.3.3	Theory–Design Space	37
3.3.4	Operation of LyoStar3	43
3.3	Result and Discussion	47
3.4.1	Evaluation of the Vial Heat Transfer Coefficient K_v	47
3.4.2	Lyophilization Cycle with a Normal and Annealing Freezing Step	48
3.4.3	Lyophilization with a Temperature-Controlled Nucleation Step	51
3.4.4	Calculation of the Design Space for the Primary Drying Stage	54
3.4.5	Verification Study for the Primary Drying Conditions Based on the Design Space	56

3.4 Conclusion	57
Chapter 4: Temperature Measurement by Sublimation Rate as a Process Analytical Technology Tool in Lyophilization	58
4.1 Introduction	58
4.2 Experimental	63
4.3 Result and Discussion	72
4.3.1 Water Vapor Transfer Resistance Coefficient through Main Pipe	72
4.3.2 Monitoring of the Product Temperature Profile at 220- and 440-Vial Scales	75
4.3.3 Validation Study at 660-Vial Scale	81
4.4 Conclusion	84
Chapter 5 General Conclusion	86
Further Perspectives	88
Acknowledgement	91
References	92
Refereed Papers	97

Chapter 1 General Introduction

In order to store drug products and foods for an extended-period of time and to maintain their storage characteristics, an appropriate drying method should be applied to remove water from the drug products and foods because it deteriorates the product quality. Various drying technologies have been developed, including the lyophilization [1], spray drying [2,3], and reduced-pressure drying [4]. In the manufacturing of pharmaceutical drug products such as unstable chemicals and sterile products, the lyophilization (also well known as freeze drying) has been widely used as an effective means [1,5]. Meanwhile, lyophilization is a time- and energy-intensive process that could take days or even weeks to finish if the freeze-drying cycle is not optimized [6-10].

In the commercial manufacturing, several thousand vials or more (several tens thousands) are lyophilized one time. Then, a failure of lyophilization did truly give a severe cost impact. Therefore, a scale-up of lyophilization at lab-scale and a transfer of lyophilization recipe to other types of equipment have been investigated in the earlier studies from the approach by the trial-and-error method [11,12]. Some researchers have proposed the practical advice for design of freeze-drying processes for pharmaceuticals [13]. However, the design based on trial-and-error experiments often causes variations in product quality and increases manufacturing costs. Thus, it is well-known that the existing scale-up theory is far from being sufficient. Then, the control method for the lyophilization process at a commercial scale needs to be improved.

In 2002, the Food and Drug Administration (FDA) announced a significant new initiative, Pharmaceutical Current Good Manufacturing Practices (CGMPs) for the 21st Century [14]. In addition, guidance on process analytical technology (PAT) to meet the 21st century challenges

was represented by FDA in 2004 [15]. In 2009, based on the agreement in the International Council for Harmonization, Technical Requirements for Pharmaceuticals for Human Use (ICH) Q8 (R2) Pharmaceutical Development was updated and the principle of quality by design (QbD) was described [16]. QbD means a systematic approach to development that begins with predefined objectives and emphasizes product and process understanding and process control, based on scientific approach and quality risk management.

The critical elements of QbD are the Design Space and Process Analytical Technology (PAT) [17]. According to “ICH Q8 Pharmaceutical Development Guidance” [16], a design space is the multidimensional combination of input variables and process parameters that have been demonstrated to provide assurance of quality. In order to proceed with the pharmaceutical development using a QbD approach, three key philosophies of Critical Quality Attributes (CQAs), Critical Process Parameters (CPPs) and Critical Material Attributes (CMAs) has been guided in the pharmaceutical industry [16,18,19]. CQAs are physical, chemical, biological, or microbiological property or characteristic that should be within an appropriate limit, range, or distribution to ensure the desired product quality [16]. CPPs are process parameters whose variability have an impact on a CQA and therefore should be monitored or controlled to ensure the process produces the desired quality [16]. CMAs are attributes of input materials whose variability has an impact on a CQA should be monitored or controlled to ensure the process produces the desired quality produces the desired quality [18]. CQAs, CPPs, and CMAs should be clarified to develop based on a QbD approach. These attributes including variables accepted so far are listed in Table 1. In accordance with the principles of ICH Q9, risk assessment to identify and rank process parameters that may impact CQAs based on scientific knowledge and experiments will be conducted, and effective control strategies will be developed to minimize the risks to acceptable levels. On the other hand, the PAT is an integral part of QbD, because the

paradigm relies on the use of real-time process monitoring and control as a part of an overall control strategy [17]. To design robust control strategies, design space and PAT are useful.

In the thesis of chapter 1, scale-up procedure for primary drying process in lyophilizer by using the vial heat transfer and the drying resistance was investigated. In the thesis of chapter 2, the impact of ice nucleation technology on the quality and the productivity was researched. In the thesis of chapter 3, scalable PAT tool to be applied to commercial lyophilization process was developed.

Table 1 Critical Material Attributes and Process Parameters, Critical Quality Attributes

Critical Material Attributes (CMAs)	Critical Process Parameters (CPPs)	Critical Quality Attributes (CQAs)
<ul style="list-style-type: none">• Glass transition temperature• Eutectic temperature• Cake collapse temperature• Product temperature• Water vapor transfer resistance of the dried layer (R_p)	<ul style="list-style-type: none">• Freezing temperature• Freezing rate• Annealing temperature/time• Primary drying temperature/pressure/time• Secondary drying temperature/pressure/time	<ul style="list-style-type: none">• Related substances• Appearance• Water content• Reconstitution time

Chapter 2 Scale-Up Procedure for Primary Drying Process in Lyophilizer by Using the Vial Heat Transfer and the Drying Resistance

2.1 Introduction

The establishment of scale-up theory requires the deeper understanding on the principle of lyophilization. The lyophilization process that is commonly used consists of three stages: (1) freezing stage, (2) primary drying stage, and (3) secondary drying stage.

- The freezing stage has been well understood in terms of physicochemical and engineering aspects. If water is used as a solvent, water turns into ice during the freezing stage to separate from other solute components. The freezing is usually completed within a few hours [20,21].
- The primary drying stage is also called as a sublimation drying stage. In this stage, the chamber pressure is reduced below the equilibrium vapor pressure of ice, and the heat will be transferred from the shelf surface to the product. This prevents the decrease in the product temperature due to sublimation and promotes sublimation. The sublimated vapor is transferred to the condenser and then turns into ice again. The heat removed from the product as a latent heat of sublimation will be supplied again from the shelf [22]. Generally, the primary drying stage lasts the longest among three stages in the lyophilization process. Optimizing and shortening this procedure can reduce the cost significantly.

- The secondary drying stage is the diffusion and desorption drying stage. It is a procedure to remove the water that did not turn into ice during the freezing phase and was captured inside the solute components as nonfreezing water. The objective of secondary drying is to reduce the final residual water content to acceptable level for stability assurance. This stage requires a higher temperature setting than the primary drying stage, but the drying is usually completed within a few hours.

In order to avoid the trial-and-error approach, the control of three stages mentioned above has been studied. Of three stages, the primary drying stage takes longest time. Therefore, the shortening of primary drying stage is always an issue in terms of economical cost at a commercial scale.

As the understanding on the lyophilization process has progressed, the mathematical models based on parameters that dominate the lyophilization process have been developed [11,12,23-25]. In recent years, the higher temperature of products and reduction of resistance of the frost layer to vapor flow results in the improvement of the primary drying efficiency [23-25].

If the product temperature rises too much during the drying stage, a collapse (improper freeze drying) of the product occurs [26]. When a bulk solution is continuously cooled down under the atmospheric pressure, the solution maintains a super-cooled state even below the freezing temperature. And the temperature increases up to around the equilibrium freezing point due to the heat of crystallization caused by the ice nucleation. When the heat is removed continuously by cooling it down, the ice crystal will grow. Moreover, water is captured in solute components, excluding the non-freezing water, will be transferred to the ice [27]. When the cryopreservation proceeds, solute components are concentrated. Once the temperature reaches

the eutectic temperature (T_e), water and solute components will become independent from each other, forming the eutectic mixture through the crystallization. Mannitol, glycine, sodium chloride, and phosphate buffer are known to crystallize during the freezing process at a certain concentration [28]. Generally, drugs or excipients that are developed to use as injection products have high affinity with water, and they rarely form eutectic crystals during the freezing process. When solute components are concentrated, below the glass-transition temperature (T_g'), they turn into amorphous solids that have a low molecular mobility. This phenomenon is called glass transition. The T_g' value can be determined by the low-temperature differential scanning calorimetry (DSC). The collapse temperature (T_c) that can be determined by the freeze-drying microscopy is also the important index of the lyophilization process. Cake collapse temperature is the temperature above which the lyophilized product loses its macroscopic structure and cake collapses during the primary drying process. Generally, it is known that T_c is approximately 2°C higher than T_g' [29]. In order to produce an acceptable lyophilized product, it is always required to perform the primary drying at the temperature lower than T_c .

Another factor for the improved efficiency of the drying is the transfer resistance of dried layer to water vapor flow. The primary drying stage is controlled by the heat transfer and the mass transfer, as illustrated schematically in Figure 1. The heat which was transferred from the heat medium to the shelf is transferred to the shelf surface. Then, the heat is transferred to the bottom of the vial via the gas (mainly vapor) that is present between the shelf surface that comes into contact with the bottom of the vial and the bottom surface of the vial that comes into contact with the shelf. During this heat transfer, the radiation heat from the walls of the lyophilizer is also transferred to the vial [30]. The heat transferred to the bottom of the vial is transferred to the sublimation interface via the frost layer, and consumed as the latent heat of sublimation. Accordingly, these heat transfers induce the conversion from ice to vapor. The

progression of ice sublimation forms the dried layer to play a role for the resistor against the sublimation, suppressing the sublimation rate. If this drying resistance (R_p : water vapor transfer resistance of the dried layer) is well controlled, the heat input to the product would be able to be controlled, and the optimal primary drying temperature will be secured.

In the practical equipment, the excess heat input troubles the lyophilization process. The radiation from the shelf and from chamber walls affects the heat transfer to the product [31]. It is the vials at the edge position that are influenced by the radiation. The production lyophilization at large scale possesses the high portion of vials at the edge position to ones at the central position than the lab-scale lyophilization. Pisano et al. proposed to place the empty vial at the edge of the shelf [24]. This recipe burden the practitioner. Generally, the preservation of the dynamics in the lyophilization between lab- and production-scale is needed for the successful scale-up, *i.e.*, the R_p values at lab- and production-scale are equivalent [23]. Meanwhile, the operating condition where the R_p values at lab- and production scale are equivalent has been still unclear. The commercial lyophilizers are strictly operated under the dust-free condition. Then, the operation of lab- and pilot-scale lyophilizer under the dust-free condition, as well as the commercial level, might meet the requirement of the equivalent dynamics.

The major objective in this research is to establish the practical scale-up procedure for primary drying process. We assumed that the R_p obtained using pilot lyophilizer under high efficiency particulate air (HEPA)-filtrated airflow condition can reflect R_p to be obtained using production under Class 100 environment condition. Firstly, the T_g' and T_c values for the target formulation were evaluated. Secondly, the vial heat transfer coefficient (K_v) for the pilot and the production lyophilizers were evaluated by using 1,008 and 6,000 vials, respectively. Thirdly, the lyophilization cycle for the formulation was performed in the pilot lyophilizer under

HEPA-filtrated air- flow condition in order to protect airborne ice-nucleating particles and R_p for the formulation was calculated using the K_v value of the pilot lyophilizer. At last, the lyophilization cycle for the commercial manufacturing was designed based on the maximum value of R_p calculated from manufacture with the pilot lyophilizer and from the vial heat transfer coefficient of the production lyophilizer, and then the cycle parameters were verified using the production lyophilizer of 60,000 vials under Class 100 production environment.

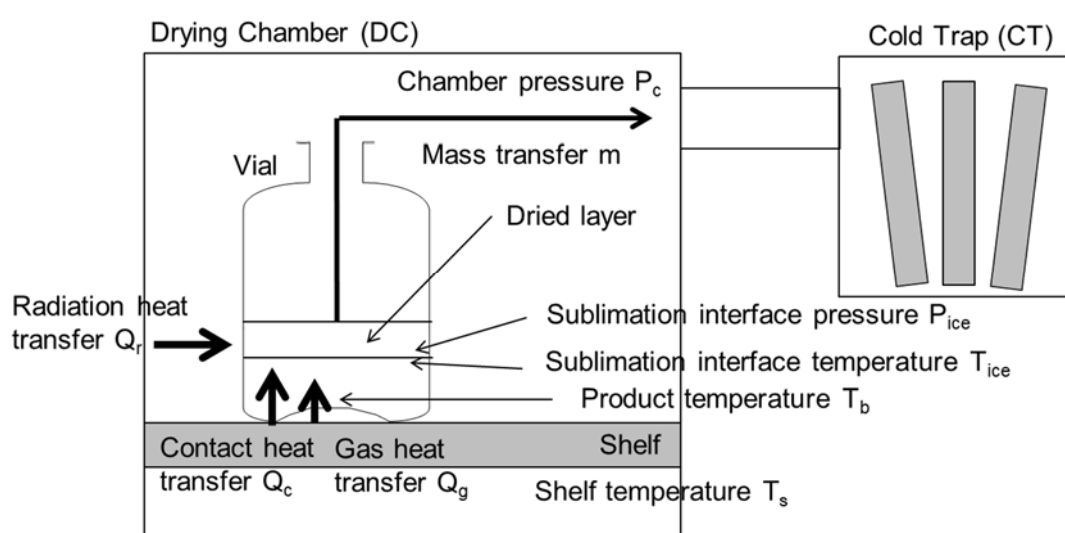


Figure 1 Schematic Illustration of Heat Transfer and Mass Transfer of Vial Near the Wall

2.2 Experimental

2.2.1 Materials

Flomoxef sodium solution for injection (molecular weight: 518.45, CAS No. 92823-03-5) was used for the investigation. The formulation included sodium chloride as stabilizing agent. The total solid content of the solution was 31% (w/w, liquid density: 1.156 g/mL), with all solid material dissolved in water for injection. The 14 mL vials manufactured from clear, colorless, round borosilicate glass tubing that meet United States Pharmacopeia (USP) criteria for Type I glass and the stoppers suitable for lyophilization manufactured from chlorinated butyl

elastomer were used for the investigation.

2.2.2 Physical Property Evaluation of Flomoxef Sodium Bulk Solution

The T_g of samples can be estimated by DSC. Thirty one percent Flomoxef sodium bulk solution was loaded into the measurement cell of the DSC (TA Instruments, Q2000). The sample was then equilibrated at -80°C to freeze the liquid and held isothermally for 30 min. Afterwards, the temperature elevated by a rate of $2^{\circ}\text{C}/\text{min}$ up to 20°C . The T_c value was determined according to the lyophilization microscopy technique by using the lyophilization microscope (Linkam Scientific Instruments, Linksys 32). The bulk solution was poured into the observation cell and equilibrated at -40°C to be frozen. This sample was kept isothermal at -40°C for 5 min. Furthermore, the atmosphere within a measurement cell approached vacuum by decreasing the pressure. After the pressure was stabilized, the temperature was elevated at a rate of $1^{\circ}\text{C}/\text{min}$ to 0°C .

2.2.3 Estimate of Vial Heat Transfer Coefficient

The schematic illustration with respect to the primary drying of vial in dry chamber is shown in Fig. 1. Lyophilizer RL-402BS (total shelf area of 1.8 m^2) manufactured by Kyowa Vacuum Engineering Co., Ltd. (KYOWAC, Japan) was utilized for the pilot scale experiments. Lyophilizer RL-4536BS (total shelf area of 36.1 m^2) manufactured by KYOWAC was utilized for the production scale experiments. 3,024 vials and 60,000 vials of 14 mL vial can be placed in the pilot lyophilizer RL-402BS and the production lyophilizer RL-4536BS, respectively. Five milliliters of water for injection was filled in the number of vials to be placed fully on at least one shelf in the lyophilizer for this evaluation (pilot lyophilizer: at least 1,008 vials, production lyophilizer: at least 6,000 vials), and the mass before lyophilization was measured.

The vials were packed tightly on the shelf (hexagonal arrangement). The freezing procedure was performed at -40°C for 4h, and the primary drying in the pilot machine was performed at 4, 10, and 20 Pa with a shelf temperature of -10°C for 7 h, and the primary drying in the production machine was performed at 2, 10, and 20 Pa with a shelf temperature of -5°C for 7 h, respectively.

In order to monitor the product temperature during the lyophilization, the thermocouples were installed in the vials and placed in the center as well as the edge of the shelf. In addition, in order to monitor the temperature of the shelf surface, the thermocouples were taped on the shelf surfaces that are located at the inlet as well as the outlet of the heat medium. The mass loss over time (dm/dt) after the lyophilization was measured to determine the amount of water used for sublimation. At last, the K_v values were calculated from the shelf surface temperature (T_s), product temperature (T_b), latent heat of ice (ΔH_s), cross sectional area of vial calculated from its outer diameter (A_v), and dm/dt , according to the following Eq. 1. See **Appendix A** for the details.

$$K_v = \frac{\Delta H_s (dm/dt)}{A_v (T_s - T_b)} \quad 2 - (1)$$

2.2.4 Evaluation of the Water Vapor Transfer Resistance of the Dried Layer

Pilot lyophilizer RL-402BS (total shelf area of 1.8 m^2) manufactured by KYOWAC was utilized for the pilot scale experiments. Prior to lyophilization, Flomoxef sodium bulk solution was filtered through a $0.2\mu\text{m}$ filter. 3.15mL of filtered Flomoxef sodium bulk solution was filled in 1008 vials to be placed fully on one shelf in the lyophilizer under HEPA-filtrated airflow condition. After filling, the vials were semi-stoppered and loaded into the lyophilizer,

and lyophilized. The freezing procedure was performed at -41.5°C , and the primary drying was performed at -10°C under 6.7 Pa pressure, and the secondary drying was performed at 50°C under 2 Pa pressure. Thermocouples were installed in the vials filled with the Flomoxef sodium solution in such a manner that the end part of the thermocouple comes in the center of the bottom of the vials. If the sensor touches the inside wall of the vial, the vial temperature will be measured, instead of the product temperature. The thermocouples were taped on the shelf surfaces that are located at the inlet as well as the outlet of the heat medium. While lyophilization was performed, the shelf temperature, the product temperature, and pressure were monitored. The point at which the product temperature increases sharply toward the established shelf temperature was determined as the drying endpoint for analysis. From the shelf surface temperature, product temperature and pressure profile, the water vapor transfer resistance of the dried layer (R_p) was calculated. From the relationship between the water in sublimation and the sublimation rate, the drying time was calculated. The procedures for the analysis are shown below.

$$R_p = \frac{A_p(P_{\text{ice}} - P_c)}{\left(\frac{dm}{dt}\right)} \quad 2 - (2)$$

2.2.5 Verification Study in the Production Lyophilizer

Lyophilizer RL-4536BS (total shelf area of 36.1 m^2) manufactured by KYOWAC was utilized for the production scale experiments. Prior to lyophilization, Flomoxef sodium bulk solution was filtered through a $0.2\mu\text{m}$ filter. 3.15mL of filtered Flomoxef sodium bulk solution was filled in 60,000 vials to be placed fully on ten shelves in the lyophilizer under Class 100 production environment. After filling, the vials were semi-stoppered and loaded into the

lyophilizer, and lyophilized. The freezing procedure was performed at -41.5°C , and the primary drying was performed at -10°C under 6.7 Pa pressure, and the secondary drying was performed at 50°C under 2 Pa pressure. Since the product temperature during the primary drying should be preferably 2°C to 5°C lower than the collapse temperature [13], the target product temperature was controlled to be -33°C to -30°C considering the collapse temperature of the Flomoxef sodium bulk solution. In order to maintain the sublimation interface temperature at -30°C or less and to prevent the cake collapse during the primary drying stage, the shelf temperature was expected to be designed at -11°C or less. In this verification study, the shelf temperature was designed at -10°C (predicted product temperature: -29°C) as a boundary condition to assure the suitability of the design for the shelf temperature of -11°C or less during primary drying stage.

2.3 Result and Discussion

2.3.1 Physical Property Evaluation of Flomoxef Sodium Bulk Solution

Collapse should be avoided over the primary drying. The glass-transition temperature (T_g) and collapse temperature (T_c) are therefore critical physical property to the primary drying. The T_g value of target solution, Flomoxef sodium solution was estimated from the DSC measurement. Figure 2(a) depicts the DSC curve for the target. A slightly decrease in heat flow observed at around -31°C was corresponding with the glass-transition. For a solute system which does not crystallize but remains amorphous, this maximum temperature is generally equivalent to the T_c value. The T_c value was measured by the freeze-drying microscope technique. Accordingly, a process of primary drying of Flomoxef sodium bulk solution was observed microscopically, as shown in Figure 2(b). At -30°C , the sublimation interface between the frozen layer and dried one was definitely observed as shown in Figure 2(b1). At

-28 °C, a partial cake collapse was observed as demonstrated in the arrow in Figure 2(b2). Furthermore, this partial collapse was, at -26 °C, spread along the sublimation interface (Figure 2(b3)). Thereby, the T_c value was determined to be -28 °C. The above results were agreed with the finding [29] that T_c is higher than T_g' by approximately 2 °C.

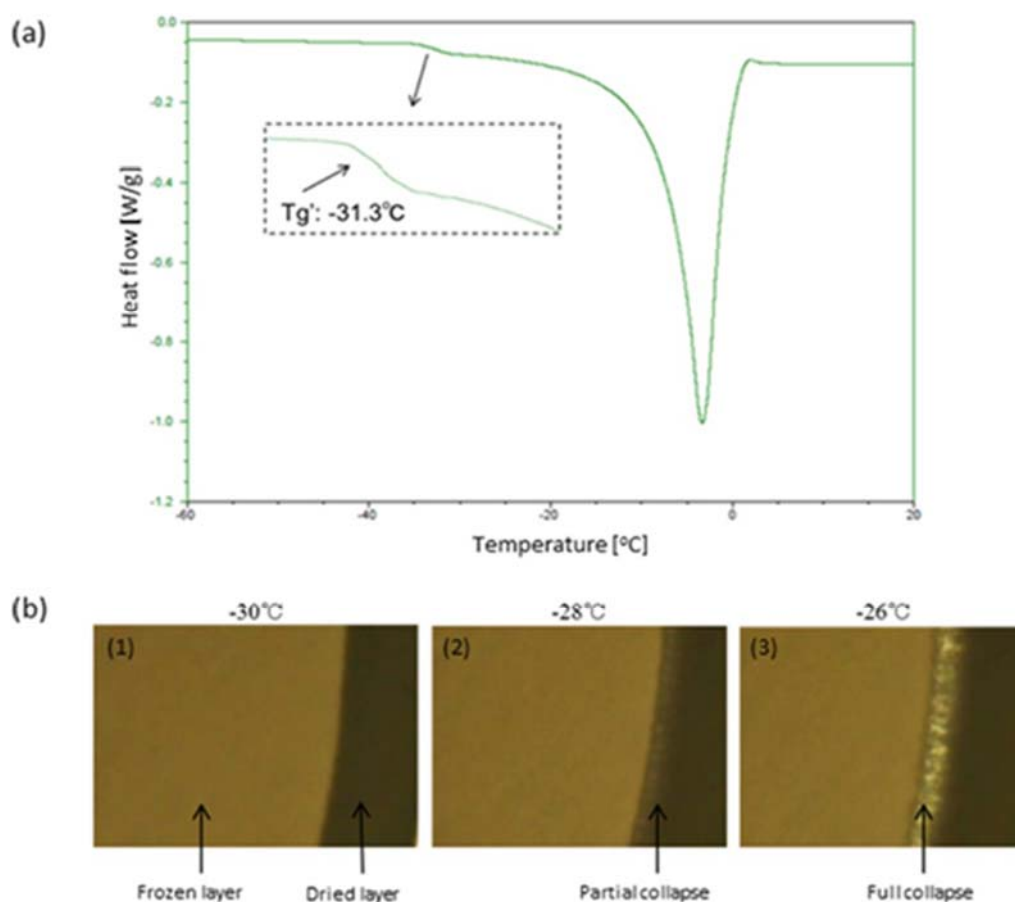


Figure 2 (a) DSC Thermograms of Flomoxef Sodium Bulk Solution and (b) Freeze Dry Microscopy Photographs of Flomoxef Sodium Bulk Solution

(1) Cake collapse was not observed in the sublimation interface at -30°C. (2) Onset of partial cake collapse was observed at -28°C. (3) Full cake collapse was observed at -26°C.

2.3.2 Comparison of Sublimation Behavior in Both Machines

The sublimation behavior in pilot lyophilizer (RL-402BS) as well as the production lyophilizer (RL-4536BS) was investigated in the primary drying process. The sublimation

behavior is subjective to be affected by the radiation heat transfer from the wall, in particular of production lyophilizer [30]. To evaluate the influence the edge and center positions of lyophilizer on the heat transfer, the sublimation behavior was investigated at only one shelf. That is to say, the sublimation amount of 1,008 of whole 3,024 vials for RL-402BS, and 6,000 of whole 60,000 vials for RL-4536BS were monitored.

Figure 3 shows the distribution of sublimation amount (m) in the both machines at the certain time under 10 Pa. The m value was 2.0 – 3.0 g at the edge position of pilot machine whereas 1.5 – 2.0 g in the center position (Figure 3(a)). In contrast, the m value was 2.0 – 3.5 g at the edge position of the production machine although the 1.5-2.5 g at the center position. It was obvious, in both the machines, that more amount of ice was sublimated at the edge position as compared with the center position. This result implied that the vial heat transfer at the edge position of the machine was strongly affected by the radiation heat input [13,23,31,32], accelerating the sublimation rate. It was considered that such a distribution of sublimation resulted from the position-dependency of heat transfer property.

Accordingly, the vial heat transfer coefficient (K_v) was estimated from equation (1). For this, the slope of dm/dt was coarsely estimated from Figure 3: *i.e.* $dm/dt = m(t)-m(0)/t$. By using $\Delta H_s = 669$ cal/g, $A_v = 4.71$ cm², the average shelf temperature (T_s) and the average product temperature (T_b) during the primary drying, the mass loss over time (dm/dt), the K_v value was estimated as shown in Table 2. At $P_c = 4$ Pa, the $10^4 K_v$ values at the edge and center positions were 3.40 ± 0.37 and 2.38 ± 0.18 cal/(s·cm²·°C), respectively. The K_v value at the edge was higher than that at the center position. This is attributed to the radiation heat transfer from the wall of machine as shown in Figure 1. In addition, the increase in chamber pressure up to 20 Pa elevated the K_v value. This attributes to the increased amount of gas (vapor) that is present in the gap between the shelf surface and the bottom of the vial. In contrast, the decrease in

chamber pressure during the primary drying stage enlarged the difference (Edge/Center) in the K_v value between the edge and center positions (from 1.27 at 20 Pa to 1.48 at 4 Pa). This occurs because the vapor amount in the chamber decreases under a highly vacuumed chamber pressure condition, which will diminish the effects of the gas heat transfer and will relatively increase the effects of radiation heat transfer. The same was true for the production machine (right column in Table 2). Furthermore, the K_v values between both machines were compared. At 10 Pa, the pilot machine indicated the K_v value is higher than the production machine, at both edge and center. The same was true for the comparison at 20 Pa. Meanwhile, the difference in Edge/Center of production machine (= 1.27) surpassed that of pilot machine (= 1.33) at 20 Pa. Thus, the scale up of lyophilizer appeared to reduce the heat transfer property of vials.

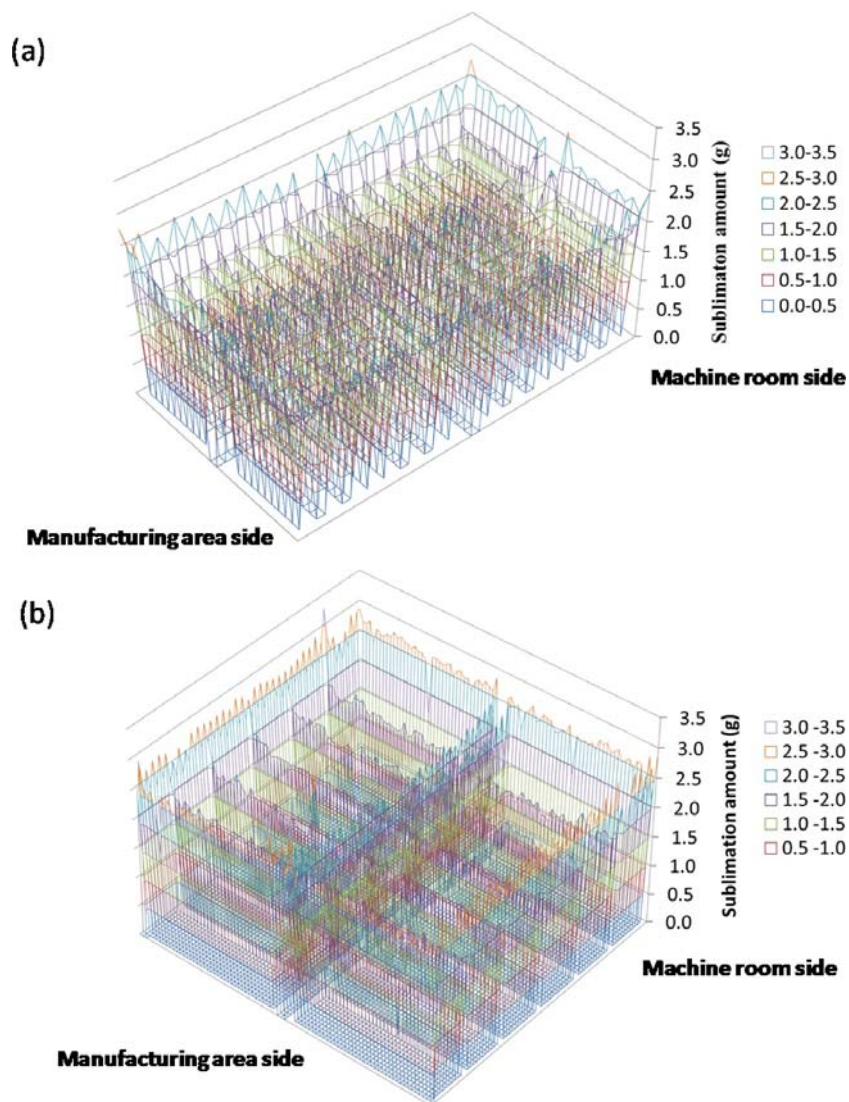


Figure 3 3D-Distribution of the Mass of Ice Sublimed in a (a) Pilot and (b) Production Lyophilizer

(a) 1,008 vials filled with WFI were used for the sublimation test. Shelf temperature, chamber pressure and primary drying time were -10°C , 10 Pa, and 7h, respectively.

(b) 6,000 vials filled with WFI were used for the sublimation test. Shelf temperature, chamber pressure and primary drying time were -5°C , 10 Pa, and 7h, respectively.

Table 2 Analysis of Vial Heat Transfer Coefficient with Pilot and Production Lyophilizer

Chamber pressure (Pa)	Pilot Machine			Production Machine		
	$10^4 K_v$ (cal/s·cm ² ·°C)			$10^4 K_v$ (cal/s·cm ² ·°C)		
	Center	Edge	Edge/Center	Center	Edge	Edge/Center
2	–	–	–	1.46 ± 0.04	2.64 ± 0.09	1.81
4	2.38 ± 0.18	3.40 ± 0.37	1.48	–	–	–
10	3.78 ± 0.26	5.17 ± 0.55	1.37	3.54 ± 0.08	4.61 ± 0.11	1.30
20	5.07 ± 0.35	6.46 ± 0.52	1.27	4.57 ± 0.10	6.10 ± 0.11	1.33

2.3.3 Contribution of Elemental Process of Heat Transfer to Vial Heat Transfer

The vial heat transfer process consists of the contact heat transfer, gas heat transfer, and radiation heat transfer. Their heat transfer coefficients were defined as K_c , K_g , and K_r , respectively. According to the previous reports [26,33], K_c and K_r do not depend on the chamber pressure (P_c) and the K_g value depends on P_c . K_g was described as a function of P_c as follows.

$$K_g = \frac{\alpha \Lambda_0 P_c}{1 + l_v \frac{\alpha \Lambda_0}{\lambda_0} P_c} \quad 2 - (3), \quad \text{where} \quad \alpha = \frac{\alpha_c}{2 - \alpha_c} \sqrt{\frac{273.2}{T}}$$

Λ_0 represents the free molecular heat conductivity of water vapor at 0°C, and λ_0 is the thermal heat conductivity of water vapor at ambient pressure, α is a function of the energy accommodation coefficient, α_c is the parameter, and T is the absolute temperature of the water vapor.

The K_v value obtained in the last section was plotted against the corresponding P_c value. The dependency of K_v on chamber pressure is theoretically written by equation (4) (See **Appendix B**).

$$K_v = a + \frac{bP_c}{1 + cP_c} \quad 2 - (4)$$

Nonlinear regression analysis of Equation (4) was performed by using $\Lambda_0 = 6.34 \times 10^{-3}$ cal/(s·cm²·°C), $\lambda_0 = 4.29 \times 10^{-5}$ cal/(s·cm·°C). Also, $\alpha_c = 0.67$ was used [26]. The results of analysis are shown in Figure 4(a). Overall, the experimental data were fitted with the theoretical curves. Approaching P_c to 0 Pa, the contribution of gas heat transfer diminished. In other words, the intercept of K_v in Figure 4(b) meant the contribution of K_c and K_r . The contribution of K_g was elevated by more than 3 times as compared with other two factors.

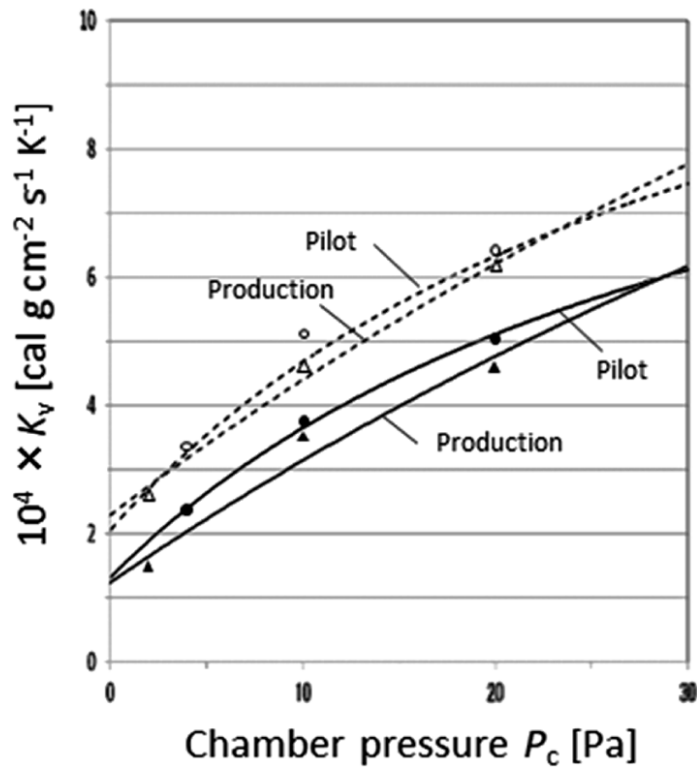


Figure 4 Dependency of Vial Heat Transfer Coefficients on Chamber Pressure with Pilot and Production Lyophilizer

Solid curves: center position; dotted curves: edge position. Experimental data: K_v values for the center position for the pilot (closed circle) and production (closed triangle); K_v values for the edge position for the pilot (open circle) and production (open triangle). The pilot

lyophilizer (RL-402BS) and Lyophilizer RL-4536BS as production machine were used to estimate K_v value at -10 and -5°C , respectively. Those curves were best fit with experimental data summarized in Table 1. The details for calculation using Eq. 4 are described in Appendix B.

2.3.4 Monitoring of Temperature Profile for Design of Operation Conditions

Another important parameter to predict the primary drying process is the water vapor transfer resistance of the dried layer (R_p). The amount of airborne particles may have impact on ice-nucleation temperature and cause larger variability in R_p , and hence the manufacture in pilot lyophilizer was implemented under HEPA-filtrated airflow condition to assume R_p to be obtained in production lyophilizer under Class 100 production environment. The dried layer generally grows dependent of the T_b value. Figure 5(a) shows the T_b -profile of the vial placed at the center position in the pilot lyophilizer during the primary and secondary drying stage, monitored by thermocouples. At $T_s = -10^\circ\text{C}$, the T_b value gradually increased to approached the constant T_b at around -30°C and represented the steady state ice sublimation, followed by a sharp increase step to the shelf temperature after 18.5 h and essentially equilibrated to the shelf temperature after 24 h. After the completion of primary drying stage, the T_b value indicated the stepwise increase accompanied with the shift of T_s up to 50°C during secondary drying stage. Based on the T_b -profile obtained during the primary drying in the pilot lyophilizer, the drying resistance (R_p) was then calculated using Equation (2). The values of parameters for calculations are as follows: $W_{\text{fill}} = 3.64$ g, $\rho_{\text{ice}} = 0.918$ g/mL, $\rho = 1.16$ g/mL, $C = 0.31$ g/g, $A_p = 3.84$ cm², $A_v = 4.71$ cm², $L_{\text{max}} = 0.73$ cm, $\Delta m_{\text{H}_2\text{O}} = 2.51$ g/vial, $\Delta H_s = 669$ cal/g, $10^4 K_v$ (at 6.7 Pa) = 3.02 cal/(s·cm²·°C). The variation of R_p as a function of dried layer thickness defined as ($L_{\text{max}} - L_{\text{ice}}$) is shown in Figure 5(b). Completing the sublimation of ice, the dried layer thickness approached to 0.73 cm (equivalent to L_{max}), at which the R_p value indicated the maximum value being 7.9 Torr·cm²·h/g at 6.7 Pa.

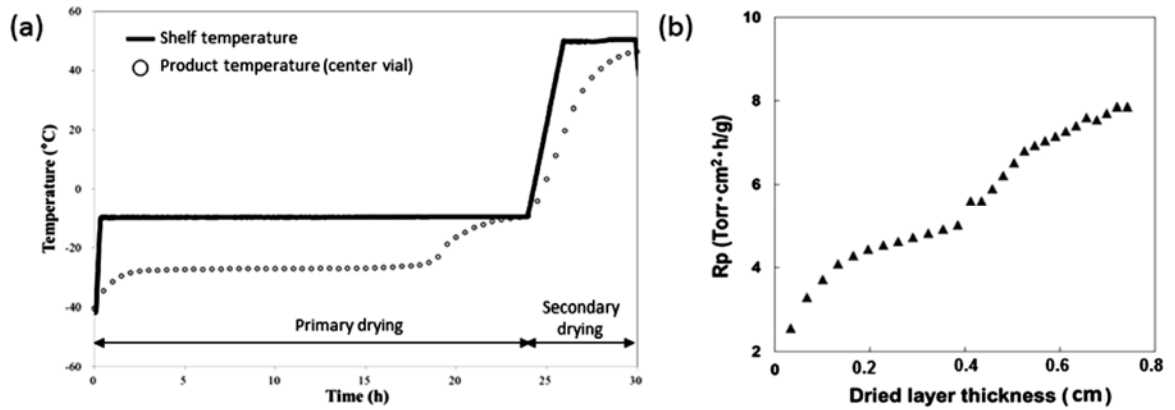


Figure 5 (a) Temperature Profile for Vial and (b) Resistance of Dried Product Layer as a Function of Time during Primary Drying

The pilot lyophilizer (RL-402BS; 1,008 vials) was used to estimate R_p value. The values of parameters are as follows: $W_{\text{fill}}=3.64$ g, $\rho_{\text{ice}}=0.918$ g/mL, $\rho=1.16$ g/mL, $C=0.31$ g/g, $A_p=3.84$ cm², $A_v=4.71$ cm², $L_{\text{max}}=0.73$ cm, $\Delta_{m\text{H}_2\text{O}}=2.51$ g/vial, $\Delta H_s=669$ cal/g, $104 K_v=3.02$ cal/(s·cm²·°C) at $P_c=6.7$ Pa. The details for calculation are described in Appendix C.

2.3.5 Scale-Up of Pilot to Production Lyophilizer

In order to produce an acceptable lyophilized product, it is always required to perform primary drying at the temperature lower than T_c . Then, the T_s in the production lyophilizer need to be designed at -5°C or less because of -28°C of the cake collapse temperature for Flomoxef sodium drug product. For this, both the sublimation interface temperature (T_{ice}) during the primary drying step and the drying time, at the production scale, can be established based on the maximum R_p value calculated from manufacture with the pilot lyophilizer (RL-402BS) and from the K_v value of the production lyophilizer (RL-4536BS). Specifically, when the R_p value is known, the design of operational variables T_s and P_c can give the T_{ice} and T_b values according to the following equation (5), followed by prediction of the drying time according to equation (2). This detailed treatment is described in **Appendix C**.

$$K_v A_v (T_s - T_{ice} - \Delta T) = \frac{0.1833 A_p}{R_p} \left(2.69 \times 10^{10} \cdot \exp \left(-\frac{6144.96}{273.15 + T_{ice}} \right) - P_c \right) \quad 2 - (5)$$

From the last section, $R_{p,max} = 7.9 \text{ Torr}\cdot\text{cm}^2\cdot\text{h/g}$ at $P_c = 6.7 \text{ Pa}$ was obtained. Thereby, the equation (5) gave the T_b and T_{ice} under the designed T_s . The predicted values were summarized in Table 3. Varying T_s from -15 to -5 °C, the T_b and T_{ice} values similarly altered from -31 to -28 °C. The corresponding time for drying operation was calculated to be ranged from 25 to 17 hours. The primary drying stage requires the occurrence of the product cake collapse. Therefore, we selected $T_s = -11 \sim 10$ °C and the needed time for primary drying stage was around $20 \sim 21$ h as the optimal condition. In this verification study, the shelf temperature was designed at -10 °C (predicted product temperature: -29 °C) as a boundary condition.

In order to establish scientific evidence that a lyophilization process is capable of consistently delivering quality product, consecutive three batches of Flomoxef sodium drug product were then manufactured in 60,000 vials scale which is the commercial scale. Lyophilizer RL-4536BS was utilized for the production scale-verification study. Visual inspection was carried out for 60,000 lyophilized vials and the yield of the three batches was 99% or more (99.6%, 99.7%, 99.3%, respectively). Acceptable lyophilized products were observed with preventing the occurrence of product cake collapses. It was considered that the obtained yield was sufficient for routine production.

Thus, the scale-up theory using combination of the vial heat transfer of lyophilizers with the resistance of dried product layer obtained under HEPA-filtrated airflow condition could bridge the gap between the pilot scale (3,024 vials) and the production scale (60,000 vials) to the extent where the product was sufficiently acceptable.

Table 3 Predicted Sublimation Interface Temperature and Drying Time for the Production Lyophilizer (Calculated Using the Maximum Drying Resistance [$R_p = 7.9$] with the Pilot Lyophilizer)

Set Value		Predicted Value		
Shelf Temperature T_s (°C)	Chamber pressure P_c (Pa)	Product Temperature T_b (°C)	Sublimation interface temperature T_{ice} (°C)	Drying Time (h)
-15	6.7	-31	-31	25
-14	6.7	-30	-31	24
-13	6.7	-30	-30	23
-12	6.7	-30	-30	22
-11	6.7	-29	-30	21
-10	6.7	-29	-29	20
-5	6.7	-28	-28	17

The values of parameters are same as ones in Figure 5(b) except $10^4 K_v$ (6.7 Pa) = 2.54 cal/(s·cm²·°C) and $R_p = 7.9$ Torr·cm²·h/g

2.4 Conclusion

The position of vials on the shelf gives their K_v value, which possibly becomes the obstacle to establish the scale-up theory for the production lyophilizer. It was first revealed that the K_v value estimated from the sublimated amount of ice at the position in the shelves (1,008 and 6,000 vials) was influenced by the radiation heat transfer from the wall of machine. We separately treated the K_v values at the edge and center positions in the shelf, which were dependent on the P_c . The R_p value was also determined by using the pilot lyophilizer (1,008 vials) under HEPA-filtrated airflow condition. From these investigations, we established the scale-up theory for the lyophilization of 60,000-vial scale. In the present theory, the K_v and R_p values are firstly determined, followed by the prediction of the target parameters T_b , T_{ice} , and the drying time during the primary drying stage. The verification study based on our predictions

demonstrated that the lyophilization of 60,000 vials succeeded in the yield of 99 % or more, thus indicating a robust operation with satisfactory. In addition, the R_p obtained using pilot lyophilizer under HEPA-filtrated airflow condition was confirmed to assume R_p to be obtained using production lyophilizer. This scale-up theory, which bridges the gap between the laboratory scale and the production scale, would enable us to perform an efficient and robust process design. A lyophilizer has a desired operational condition where chamber pressure cannot be controlled (*i.e.* choked flow limit) in a highly vacuumed condition or at an accelerated sublimation rate. By taking these factors into consideration, the desired operational condition where the product quality is not damaged, and at the same time, where stable manufacturing can be performed is expected to be established (*i.e.* design space) [34]. Our scale-up theory would give a certain impact on the determination of design space.

2.5 Appendix A Elucidation of K_v Based on the Heat/Mass Transfer

The heat transfer to the product during the primary drying consists of three types of heat transfer [20]. The first one is the contact heat transfer (Q_c) from the surface that directly comes into contact with the shelf as well as the bottom of the vial. The second one is the gas heat transfer (Q_g) via the gas (mainly vapor) that is present in the gap between the shelf surface and the bottom of the vial. The third one is the radiation heat transfer (Q_r). When a vial is used as a container, the gas heat transfer is estimated as the main heat transfer [35]. However, compared to the vial that is placed in the center of the lyophilizer, the vial placed at the edge of the lyophilizer has a faster sublimation rate. This indicates that the effects of the radiation heat transfer cannot be ignored [31]. In addition, the gas heat transfer depends on the chamber pressure. When the chamber pressure decreases, the gas heat transfer increases. When the

chamber pressure is over 13.3 Pa, the gas heat transfer becomes the most dominant of the 3 types of heat transfer: a contact heat transfer coefficient, gas heat transfer coefficient, and radiation heat transfer coefficient [36]. Accordingly, we estimated the gas heat transfer by using the vial heat transfer coefficient (K_v) as follows.

The heat transfer caused by the difference between the shelf surface temperature and the product temperature is shown in Equation (A1). The conversion from the heat transfer to the material transfer by sublimation is shown in Equation (A2).

$$\frac{dQ}{dt} = K_v A_v (T_s - T_b) \quad 2 - (A1)$$

$$\frac{dQ}{dt} = \Delta H_s \frac{dm}{dt} \quad 2 - (A2)$$

Both Equations (A1) and (A2) yielded the equation (1) to determine the K_v value.

$$K_v = \frac{\Delta H_s (dm/dt)}{A_v (T_s - T_b)} \quad 2 - (1)$$

By using equation (1), the K_v value can be estimated based on the heat / mass transfer.

2.6 Appendix B Decomposition of K_v into Elemental Factors

The vial heat transfer process consists of the contact heat transfer, gas heat transfer, and radiation heat transfer. Their heat transfer coefficients are defined as K_c , K_g , and K_r , respectively. The relationship among them were then given as $K_v = K_c + K_g + K_r$, according to the previous report [5]. In details, as shown in Figure 1, the heat flow into a vial from the outside

corresponds three heat flows: (i) the contact heat transfer (Q_c) from the surface that directly comes into contact with the shelf as well as the bottom of the vial; (ii) the gas heat transfer (Q_g) via the gas (mainly vapor) that is present in the gap between the shelf surface and the bottom of the vial; (iii) the radiation heat transfer from the shelf and wall (Q_r). That is to say,

$$\frac{dQ}{dt} = \frac{dQ_c}{dt} + \frac{dQ_g}{dt} + \frac{dQ_r}{dt} \quad 2 - (B1)$$

Three different heat flows may be considered to be driven by the *same* temperature difference ($T_s - T_b$), assuming the vial far from the wall; i.e. the contribution of radiation heat transfer from the wall being negligible. Therefore, each heat balance equation can be described as follows.

$$\frac{dQ_c}{dt} = K_c A_v (T_s - T_b) \quad 2 - (B2)$$

$$\frac{dQ_g}{dt} = K_g A_v (T_s - T_b) \quad 2 - (B3)$$

$$\frac{dQ_r}{dt} = K_r A_v (T_s - T_b) \quad 2 - (B4)$$

Equations (A1) and (B2) to (B4) are substituted into (B1) yields the following equation.

$$K_v A_v (T_s - T_b) = K_c A_v (T_s - T_b) + K_g A_v (T_s - T_b) + K_r A_v (T_s - T_b) \quad 2 - (B5)$$

Then,

$$K_v = K_c + K_g + K_r \quad 2 - (B6)$$

Thus, K_v can be decomposed into three elemental factors. Defining as $a = K_c + K_r$, $b = \alpha \Lambda_0$, and $c = lv (\alpha \Lambda_0 / \lambda_0)$,

$$K_v = a + \frac{bP_c}{1 + cP_c} \quad 2 - (4)$$

2.7 Appendix C Prediction of T_b and T_{ice} for Verification Test

The mass transfer is generated from the difference between the equilibrium vapor pressure of ice (P_{ice}) on the sublimation interface and the vacuum pressure (P_c) in the lyophilizer, and the resistance (R_p) of the dried layer on the sublimation interface determines the sublimation rate [22]. In actual, there is a resistance of the rubber stopper. Since this resistance is, however, extremely small compared to the drying resistance, it can be ignored. The relational expression is shown using Equation (C1).

$$\frac{dm}{dt} = \frac{A_p(P_{ice} - P_c)}{R_p} \quad 2 - (C1)$$

When Equation (B1) is converted, the drying resistance (R_p) is shown using Equation (2). The required drying time can be calculated from the integration of equation (2).

$$R_p = \frac{A_p(P_{ice} - P_c)}{(dm/dt)} \quad 2 - (2)$$

The conversion factor between the heat flow (dQ/dt) and the mass of substance (m) can be expressed using Equation (C2). The conversion factor used herein is to be 0.1833 as previously reported [26]. The term dm/dt is the sublimation rate in g/h, and the coefficient 0.1833 is the factor to convert the sublimation rate of pure water from g/h to cal/s.

$$\frac{dQ}{dt} = 0.1833 \frac{dm}{dt} \quad 2 - (C2)$$

The thickness of the maximum frozen layer is defined as L_{max} . Thereby, the thickness of the frost layer (L_{ice}) can be shown using Equation (C3).

$$L_{ice} = L_{max} \left(1 - \frac{\Delta m}{\Delta m_{H_2O}} \right) \quad 2 - (C3)$$

Assuming the percentage of the ice deposit in solutes as ε , L_{max} can be defined as follows.

$$L_{max} = \frac{\Delta m_{H_2O}}{\rho_{ice} A_p \varepsilon} \quad 2 - (C4)$$

Since the heat quantity (dQ/dt) that was supplied from the shelf surface to the product is transferred to the sublimation interface via the frozen layer. The sublimation interface temperature (T_{ice}) can be expressed in Equation (C5).

$$T_{ice} = T_b - \frac{dQ}{dt} \frac{L_{ice}}{A_v K_{ice}} \quad 2 - (C5)$$

Furthermore, from Equation (A1) and Equation (C5), T_{ice} can be expressed in Equation (C6).

$$T_{ice} = T_s - \frac{1}{A_v} \frac{dQ}{dt} \left(\frac{1}{K_v} + \frac{L_{ice}}{K_{ice}} \right) \quad 2 - (C6)$$

On the other hand, if the difference between the product temperature (T_b) and T_{ice} is expressed in Equation (C7) [36-38], T_{ice} can also be calculated using Equation (C8).

$$\Delta T = \frac{\frac{24.7L_{ice}}{A_p} \left(\frac{dm}{dt} \right)_i - 0.0102L_{ice}(T_{s,i} - T_{ice,i})}{1 - 0.0102L_{ice}} \quad 2 - (C7)$$

$$T_{ice} = T_b - \Delta T \quad 2 - (C8)$$

The sublimation interface pressure (P_{ice}) is expressed in Equation (C9), by substituting this formula into Equation (2), the R_p value at a specific time can be calculated.

$$P_{ice} = 2.69 \times 10^{10} \cdot \exp\left(-\frac{6144.96}{273.15 + T_{ice}}\right) \quad 2 - (C9)$$

In addition, from Equation (C1) and Equation (C2), Equation (C10) can be elucidated.

$$K_v A_v (T_s - T_b) = 0.1833 \frac{A_p (P_{ice} - P_c)}{R_p} \quad 2 - (C10)$$

Furthermore, a substitution of equations (C8) and (C9) into equation (C10) give equation (5).

$$K_v A_v (T_s - T_{ice} - \Delta T) = \frac{0.1833 A_p}{R_p} \left(2.69 \times 10^{10} \cdot \exp \left(-\frac{6144.96}{273.15 + T_{ice}} \right) - P_c \right) \quad 2 - (5)$$

When the R_p value is known, the design of shelf temperature (T_s) and chamber pressure (P_c) can give the T_{ice} and T_b values.

Chapter 3: Effect of Controlled Nucleation of Ice Crystals on the Primary Drying Stage during Lyophilization

3.1 Introduction

The lyophilization process that is commonly used consists of three stages: (1) freezing, (2) primary drying, and (3) secondary drying. If water is used as a solvent, then during the freezing stage, water will change to ice, separated from other solute components, and freezing will typically be completed within a few hours [20,21]. When water is cooled by atmospheric pressure, it does not voluntarily freeze at the equilibrium freezing temperature (0 °C), and it continues to maintain its liquid form below 0 °C. This is termed supercooling. In the case of purified water free of foreign particles or impurities, it can continuously supercool to approximately -48 °C [39]. Because injectable products are manufactured in a dust-free environment, they generally can continuously supercool up to approximately -20 °C [40]. The degree of supercooling is dependent on the characteristics of the formulation and freezing conditions.

The freezing stage, which determines the degree of variations in productivity and product quality, is among the most critical stages during the lyophilization process. Because water does not voluntarily freeze and maintains its supercooled state, the freezing temperature cannot be directly controlled. When the freezing temperature is high (a lower degree of supercooling), the size of ice crystals formed increases; when the freezing temperature is low (higher degree of supercooling), the size of ice crystals formed decreases. The larger the size of ice crystals, the higher the primary drying efficiency. A study reported that vials with product temperature sensors tend to have a higher freezing temperature than those without sensors, and therefore,

their sublimation rate will accelerate, causing variations in the drying endpoint [41]. According to another study, if the freezing temperature determines the sublimation rate, and if the freezing temperature can be increased by 1 °C, the primary drying time can be shortened by 3% [40]. However, the size of ice crystals determines the size of the specific surface area. In addition, the size of the specific surface area determines the diffusion and desorption rate during the secondary drying stage [13,42]. If the freezing temperature is high, the size of the ice increases, and the specific surface area decreases. A study reported that this causes the secondary drying efficiency to decrease, increasing the moisture residue in the finished product [20]. From the aforementioned discussion, it can be concluded that controlling the freezing temperature during the freezing stage is the key to designing a robust drying process.

In recent years, various ice nucleation techniques have been developed, and there are some scientific reports that have evaluated the advantages and disadvantages of these techniques [43,44]. The pressurization and depressurization technique is a promising ice nucleation control method. With pressurization and depressurization, the lyophilizer is pressurized to 0.28–0.29 MPa and quickly depressurized to 0.11 MPa (within 3 s) to form an ice nucleus on the surface of the liquid in vials [45]. For this technique, nitrogen or argon gas is used for pressurization. The mechanism of ice nucleation has not yet been clarified; however, it has been reported that the main driving forces for ice nucleation are considered to be the vibrational disturbance caused by sudden depressurization, the cooling of the liquid surface by cold gas contact, and local evaporation on the liquid surface during the sudden depressurization [46].

Once the vial heat transfer coefficient (which is dependent on the dry chamber pressure) and the drying resistance (R_p) are determined, both the sublimation interface temperature and the drying time (sublimation rate) during the primary drying stage can be predicted [23,24,47]. The region where the product quality is not damaged, and at the same time, where stable

manufacturing can be performed is expected to be established. The regions constructed in line with the aforementioned idea are termed *design spaces*. However, stable operation has been performed at a practical level to tolerate the quality variations that occur during the freezing stage. Accordingly, a larger design space has been used to afford excess safety factors. The wide range of both the sublimation interface temperature and the drying time (sublimation rate) often causes variations in the size of ice crystals. If the ice nucleation can be controlled during the primary drying stage of the lyophilization process, the area of the practical design space would be more robust.

The major objective of this study was to verify the efficacy of the improved design space combined with the controlled nucleation of ice crystals. Using the pressurization and depressurization technique, we controlled the ice nucleation of target formulation during the freezing stage. We investigated the effect of the ice nucleation control on the robust design space during the primary drying stage. Finally, a verification study was performed.

3.2 Experimental

3.3.1 Materials

Flomoxef sodium solution for injection (molecular weight: 518.45, CAS No. 92823-03-5) was used for the investigation. The formulation included sodium chloride as a stabilizing agent. The total solid content of the solution was 31% (w/w, liquid density: 1.156 g/mL), with all solid material dissolved in the water for injection. The 14-mL vials were manufactured from clear, colorless, round borosilicate glass tubing that met USP criteria for Type I glass and stoppers suitable for lyophilization were manufactured from chlorinated butyl elastomer and were used during the investigation. The physical properties of the

Flomoxef sodium bulk solution are as follows: freezing temperature: -3.3 °C; glass-transition temperature: -31 °C; and cake collapse temperature: -28 °C.

3.3.2 Analytical Procedure

The water content of the lyophilized cakes was determined using the Karl Fischer (Kyoto Electronics Manufacturing, MKS-510N) coulometric titration method. Three samples of each lot were used for the evaluation. The specific surface area (SSA) of the lyophilized samples was obtained from Brunauer–Emmett–Teller [BET] specific surface area analysis. A BET surface area analyzer (TriStar3000, Micromeritics Instrument Corporation) was used to measure the SSA. Outgassing of the samples was performed by heating the sample on a heating mantle at 40 °C for 1 h under reduced pressure. Nitrogen gas was introduced into the sample as the adsorbate. The equilibration interval was set as 5 s. Three samples of each lot were used for the evaluation. A scanning electron microscope (SEM; VE-8800, KEYENCE Corporation) was used to examine the morphologies of the lyophilized samples. The microscope scanned across the surface of the samples using an ultrafine beam of electrons at an acceleration voltage of 2–20 kV. The images of the sample surfaces were displayed at a magnification of 100 times.

3.3.3 Theory–Design Space

Heat transfer to the product during the primary drying consists of three types of heat transfer [33]. The first is contact heat transfer from the surface that directly comes into contact with the shelf as well as the bottom of the vial. The second is gas heat transfer through the gas between the shelf surface and the bottom of the vial. The third is radiant heat transfer. When a

vial is used as a container, the gas heat transfer is estimated as the main heat transfer. However, compared to the vial that is placed in the center of the lyophilizer, the vial placed at the edge of the lyophilizer has a faster sublimation rate [23,24,33,47,48]. This indicates that the effects of radiation heat transfer cannot be ignored [48]. In addition, the gas heat transfer depends on the chamber pressure. When the chamber pressure decreases, the gas heat transfer increases. When the chamber pressure is greater than 13.3 Pa, gas heat transfer becomes the most dominant heat transfer of the three [36]. Accordingly, we estimated the gas heat transfer by using the vial heat transfer coefficient (K_v) as follows.

Heat transfer (dQ/dt) caused by the temperature difference between the shelf surface temperature (T_s) and the product temperature (T_b) is related to K_v and A_v [cm^2], i.e., the cross-sectional area of the vial calculated from the vial outer diameter as follows:

$$\frac{dQ}{dt} = K_v A_v (T_s - T_b) \quad 3 - (1)$$

The relationship between the heat transfer and the material transfer via sublimation (dm/dt) is as follows:

$$\frac{dQ}{dt} = \Delta H_s \frac{dm}{dt} \quad 3 - (2)$$

where ΔH_s [cal/g] is the latent heat of sublimation. Both Equations (1) and (2) yielded the Equation (3) to determine the K_v value as follows:

$$K_v = \frac{\Delta H_s(dm/dt)}{A_v(T_s - T_b)} \quad 3 - (3)$$

The heat transfer coefficients of the contact heat, gas heat, and radiant heat transfer were defined as K_c , K_g , and K_r , respectively. According to previous reports [41,44], K_c and K_r do not depend on the chamber pressure (P_c) and the K_g value depends on P_c as is described by the function $K_g = bP_c/(1 + cP_c)$ (b and c are the positive constant). Then, $K_v (=K_c + K_g + K_r)$ can be represented as follows:

$$K_v = a + \frac{bP_c}{1 + cP_c} \quad 3 - (4).$$

This relationship between K_v and P_c has often been used in the operational design of lyophilization [23,24,47]. The mass transfer is generated from the difference between the equilibrium vapor pressure of the ice on the sublimation interface (P_{ice}) and P_c in the lyophilizer, and the resistance of the dried layer on the sublimation interface (R_p) determines the sublimation rate [33]. In addition, the resistance of a rubber stopper, which is extremely small compared to the drying resistance, is negligible. Accordingly, the relational expression is shown using Equation (5):

$$\frac{dm}{dt} = \frac{A_p(P_{ice} - P_c)}{R_p} \quad 3 - (5)$$

From Equation (5), the drying resistance (R_p) is obtained as Equation (6). The required drying time can be calculated from the integration of Equation (6).

$$R_p = \frac{A_p(P_{ice} - P_c)}{(dm/dt)} \quad 3 - (6)$$

The conversion factor between the heat flow (dQ/dt) and the mass of substance (m) can be expressed using Equation (7). The conversion factor used herein is 0.1833 as previously reported [26]. Term dm/dt is the sublimation rate in g/h, and the coefficient 0.1833 is the factor to convert the sublimation rate of the pure water from g/h to cal/s as follows:

$$\frac{dQ}{dt} = 0.1833 \frac{dm}{dt} \quad 3 - (7)$$

The thickness of the maximum frost layer (corresponding to the mass of water Δm_{H_2O}) is defined as L_{max} . Thereby, the thickness of the frost layer (L_{ice}) can be expressed as Equation (8):

$$L_{ice} = L_{max} \left(1 - \frac{\Delta m}{\Delta m_{H_2O}} \right) \quad 3 - (8)$$

Assuming the percentage of the ice deposit in solutes is ε , L_{max} can be defined as follows:

$$L_{max} = \frac{\Delta m_{H_2O}}{\rho_{ice} A_p \varepsilon} \quad 3 - (9)$$

Because the heat quantity (dQ/dt) that was supplied from the shelf surface to the product is transferred to the sublimation interface via the frost layer, the sublimation interface temperature

(T_{ice}) can be expressed by Equation (10) as follows:

$$T_{ice} = T_b - \frac{dQ}{dt} \frac{L_{ice}}{A_v K_{ice}} \quad 3 - (10)$$

Furthermore, from Equation (1) and Equation (10), the sublimation interface temperature (T_{ice}) can be expressed as Equation (11) as follows:

$$T_{ice} = T_s - \frac{1}{A_v} \frac{dQ}{dt} \left(\frac{1}{K_v} + \frac{L_{ice}}{K_{ice}} \right) \quad 3 - (11)$$

$\Delta T (= T_b - T_{ice})$ is defined similar to Equation (12). Its substitution into Equation (10) yields Equation (13). Furthermore, the substitution of Equations (5) and (13) into Equation (2) provides Equation (14) [37,38,49] in which the value of 3600 originates from the conversion of seconds to hours as follows:

$$\Delta T = T_b - T_{ice} \quad 3 - (12)$$

$$\frac{dQ}{dt} = \frac{\Delta T L_{ice}}{A_v K_{ice}} \quad 3 - (13)$$

$$\Delta T = \frac{\Delta H_s A_p L_{ice} (P_{ice} - P_c)}{3600 A_v K_{ice} R_p} \quad 3 - (14)$$

where T_{ice} is related to P_{ice} as shown in Equation (15):

$$T_{ice} = \frac{-6144.96}{\ln(P_{ice}) - 24.01849} \quad 3 - (15)$$

Eventually, P_{ice} is expressed as Equation (16), by substituting this formula into Equation (2), the drying resistance (R_p) at a specific time can be calculated as follows:

$$P_{ice} = 2.69 \times 10^{10} \cdot \exp\left(-\frac{6144.96}{273.15 + T_{ice}}\right) \quad 3 - (16)$$

In addition, the use of Equations (1), (5), and (7) yields Equation (17) as follows:

$$K_v A_v (T_s - T_b) = 0.1833 \frac{A_p (P_{ice} - P_c)}{R_p} \quad 3 - (17)$$

Furthermore, the substitution of both Equations (12) and (16) into Equation (17) provides Equation (18) as follows:

$$\begin{aligned} & K_v A_v (T_s - T_{ice} + \Delta T) \\ &= \frac{0.1833 A_p}{R_p} \left(2.69 \times 10^{10} \cdot \exp\left(-\frac{6144.96}{273.15 + T_{ice}}\right) - P_c \right) \quad 3 - (18) \end{aligned}$$

When the R_p value is known, the design of T_s and P_c can provide T_{ice} and T_b values.

3.3.4 Operation of LyoStar3

Lyophilizer LyoStar 3 (total shelf area of 0.46 m²), manufactured by SP Scientific (Stone Ridge and Gardiner, NY, USA), was utilized during this investigation. The maximum allowable vial number of LyoStar 3 is 726 vials for a 14-mL vial. We used this equipment in the following five manners.

3.3.4.1 To Estimate the Vial Heat Transfer Coefficient

First, 5 mL of water for injection was poured into 242 vials to be placed fully on one shelf in the lyophilizer for this evaluation, and the mass before lyophilization was measured. The vials were tightly packed on the shelf (hexagonal arrangement). The thermocouples were installed in the vials and placed in the center as well as the edge of the shelf to monitor the product temperature during lyophilization. In addition, to monitor the temperature of the shelf surface, the thermocouples were taped onto the shelf surfaces at the inlet as well as the outlet of the heat medium. For the container, 14-mL glass vials were used and filled with 5 mL of water for injection, and then lyophilized. The freezing procedure was performed at -40 °C, and the primary drying was performed at -5 °C under three pressure conditions: 5, 13, and 20 Pa. The mass after the lyophilization was measured and the amount of water used for sublimation was determined. From the shelf surface temperature, product temperature, and sublimation amount during lyophilization, the vial heat transfer coefficient was then calculated using Equation (3).

3.3.4.2 To Estimate the Water Vapor Transfer Resistance of the Dried Layer

Prior to lyophilization, Flomoxef sodium bulk solution was filtered through a 0.2- μ m filter. Then, 3.15 mL of filtered Flomoxef sodium bulk solution was poured into 242 vials to be placed fully on one shelf in the lyophilizer. After filling, the vials were semi-stoppered and

loaded into the lyophilizer and lyophilized. The detailed lyophilization conditions are presented in Table 4. Thermocouples were installed in the vials filled with the Flomoxef sodium solution in such a manner that the end part of the thermocouple is in the center of the bottom of the vials. If the sensor touches the inside wall of the vial, the vial temperature will be measured, instead of the product temperature. The thermocouples were taped onto the shelf surfaces at the inlet as well as the outlet of the heat medium. During the lyophilization, the shelf temperature, product temperature, and pressure were monitored. The point at which the product temperature sharply increases toward the established shelf temperature was determined as the drying endpoint for analysis. From the shelf surface temperature, product temperature and pressure profile, the water vapor transfer resistance of the dried layer (R_p) and the drying time were calculated using Equation (6).

3.3.4.3 For Lyophilization Procedures with a Normal and Annealed Freezing Step

Lyophilizer LyoStar 3 (total shelf area of 0.46 m²), manufactured by SP Scientific, was utilized for the experiments. Three lots (Lots 01, 02, and 03) of manufacturing were performed. Prior to lyophilization of each lot, Flomoxef sodium bulk solution was filtered through a 0.2- μ m filter. Then, 3.15 mL of filtered Flomoxef sodium bulk solution was poured into 242 vials to be placed fully on one shelf in the lyophilizer. After filling, the vials were semi-stoppered and loaded into the lyophilizer and lyophilized.

The detailed lyophilization conditions for Lot 01 to Lot 03 are presented in Table 4. In short, Lot 01 of the Flomoxef sodium bulk solution was cooled to 5 °C for 1 h, and then frozen. The freezing procedure was performed at -41.5 °C for 2 h. The primary drying was performed at -25 °C at 6.7 Pa. The secondary drying was then performed at 50 °C at 2 Pa. Lot 02 of the bulk solution was cooled to 5 °C for 1 h and then cooled to -5 °C for 1 h to improve the homogeneity of the ice crystallization. The freezing, primary drying, and secondary drying

procedures were the same as those of Lot 01. The freezing drying cycle for Lot 03 was the same as that of Lot 02 except for the annealing step. The annealing step was designed at 0 °C for 0.5 h to keep the product temperature below the freezing temperature, which was -3.3 °C.

3.3.4.4 For verification Study for the Primary Drying Conditions Calculated Using the Design Space

Two lots (Trials 1 and 2) of manufacturing were performed to verify the primary drying conditions calculated using the design space. Prior to lyophilization of each lot, Flomoxef sodium bulk solution was filtered through a 0.2- μ m filter. Then, 3.15 mL of filtered Flomoxef sodium bulk solution was poured into 726 vials to be placed fully on three shelves in the lyophilizer. After filling, the vials were semi-stoppered and loaded into the lyophilizer.

The detailed lyophilization conditions for Trials 01 and 02 are presented in Table 4. Trial 01 of the Flomoxef sodium bulk solution was cooled to 5° C for 1 h and then cooled to -5 °C for 1.5 h without ice formation. Following the completion of the precooling, the chamber was pressurized with nitrogen gas from 0.28 to 0.29 MPa, and then the chamber was depressurized to 0.11 MPa in 3 s or less. The shelf temperature was maintained at -5 °C for 20 min. Following the pressurization and depressurization step, the shelf temperature was reduced to -41.5 °C at 1 °C/min and held for 2 h, and the primary and the secondary drying were performed at -10 °C under 6.7 Pa of pressure and at 50 °C under 2 Pa of pressure, respectively. Trial 02 of the Flomoxef sodium bulk solution was cooled to 5 °C for 1 h and then cooled to -5 °C for 1 h. Subsequently, the shelf temperature was reduced to -41.5 °C at 1 °C/min and held for 2 h. Following this, the shelf temperature was set to 0 °C for 0.5 h as an annealing step. Primary and secondary drying were performed under the same conditions as those of Trial 01.

Table 4 Lyophilization Conditions with and without Ice Nucleation Control

Step	Parameters	Lot 01	Lot 02	Lot 03	Trial 01	Step	Parameters	Lot 04	Lot 05	Lot 06	Trial 02
Pre-cooling 1	Temperature (°C)	5	5	5	5	Pre-cooling 1	Temperature (°C)	5	5	5	5
	Time (hr)	1	1	1	1		Time (hr)	1	1	1	1
Pre-cooling 2	Temperature (°C)	—	-5	-5	-5	Pre-cooling 2	Temperature (°C)	-5	-5	-5	-5
	Time (hr)	—	1	2	1		Time (hr)	1.5	1.5	1.5	1
Freezing	Freezing Rate (°C/min)	1	1	1	1	Pressurization and depressurization	Temperature (°C)	-5	-5	-5	-5
	Temperature (°C)	-41.5	-41.5	-41.5	-41.5		Time (min)	20	20	20	20
	Time (hr)	2	2	2	2		Freezing Rate (°C/min)	1	0.5	0.1	1
Annealing	Temperature (°C)	—	—	0	0	Freezing	Temperature (°C)	-41.5	-41.5	-41.5	-41.5
	Time (hr)	—	—	0.5	0.5		Time (hr)	2	2	2	2
Re-freezing	Temperature (°C)	—	—	-41.5	-41.5	Primary Drying	Temperature (°C)	-25	-25	-25	-10
	Time (hr)	—	—	2	2		Pressure (Pa)	6.7	6.7	6.7	6.7
Primary Drying	Temperature (°C)	-25	-25	-25	-25		Time (hr)	48	58	52	48
	Pressure (Pa)	6.7	6.7	6.7	6.7	Temperature (°C)	50	50	50	50	
	Time (hr)	57	52	54	48	Pressure (Pa)	2	2	2	2	
Secondary Drying	Temperature (°C)	50	50	50	50	Secondary Drying	Time (hr)	4	4	4	4
	Pressure (Pa)	2	2	2	2		Temperature (°C)	50	50	50	50
	Time (hr)	4	4	4	4		Pressure (Pa)	2	2	2	2
Secondary Drying	Temperature (°C)	50	50	50	50	Secondary Drying	Time (hr)	4	4	4	4
	Pressure (Pa)	2	2	2	2		Temperature (°C)	50	50	50	50
Secondary Drying	Temperature (°C)	50	50	50	50	Secondary Drying	Pressure (Pa)	2	2	2	2
	Time (hr)	4	4	4	4		Time (hr)	4	4	4	4

3.3 Result and Discussion

3.4.1 Evaluation of the Vial Heat Transfer Coefficient K_v

The dependency of the chamber pressure on K_v was first determined. The sublimation rate dm/dt at different P_c values was measured to provide the K_v value using Equation (3). The resulting K_v values are summarized in Table 5. At each P_c , the K_v value at the edge position was higher than that at center position. Thus, the K_v value depended on the position of the vials on the shelf in agreement with previous reports [23,24,47]. The higher K_v value of the vials at the edge position relative to the vials at the center position originated from the contribution of radiant heat transfer from the wall to the vial. At both positions, the K_v value increased with increasing P_c . This resulted from the gas heat transfer through the gas between the bottom of the vial and the surface of the shelf.

These data were then analyzed using a nonlinear regression analysis with Equation (4) [26,33]. The results of the analysis are shown in Figure 6. The regressed parameters a , b , and c indicated a positive value in agreement with the definition of the three parameters. Based on the results of this analysis, the K_v value under each P_c value can be predicted.

Table 5 Analysis of the Vial Heat Transfer Coefficient with the Lyophilizer

Chamber pressure P_c (Pa)	$10^4 K_v$ (cal/s·cm ² ·°C)	
	Center	Edge
5	2.28	3.76
13	3.45	5.24
20	4.14	6.59

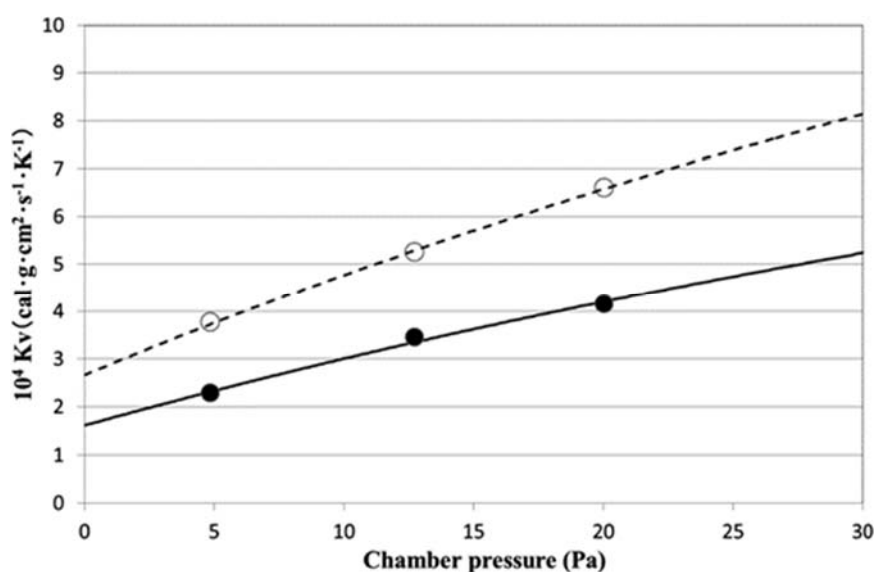


Figure 6 Dependency of the Vial Heat Transfer Coefficients (K_v) on Chamber Pressure with the Lyophilizer

Solid line: calculated K_v at the center position; dotted line: calculated K_v at the edge position; ●: measured K_v at the center position; ○: measured K_v at the edge position. Regressed parameters are $a=0.00027$; $b=0.00304$; $c=1.10348$ at the edge position and $a=0.00016$; $b=0.00201$; $c=1.10351$ at the center position.

3.4.2 Lyophilization Cycle with a Normal and Annealing Freezing Step

To discuss the ice crystal size, the SSA and water content were examined. This is because larger ice crystals form in the larger pores of the dried cakes and the larger pores can reduce the resistance to flow of the water vapor during the primary drying stage. The larger pores of the dried cakes result in a smaller SSA. The SSA value and the water content of Lots 01 to 03 after their lyophilization are summarized in Table 6. The SSA value of Lot 02 was smaller than that of Lot 01. It was considered that the precooling of 02 (cooling condition of $-5\text{ }^{\circ}\text{C}$ before the initiation of freezing as shown in Table 1) improved the heterogeneity of ice crystallization and formed larger ice crystals. The SSA value of Lot 03 was smaller than that of Lot 02. The difference between Lot 02 and Lot 03 was the annealing at $0\text{ }^{\circ}\text{C}$ for 0.5 h. Therefore, the reduction in the SSA value of Lot 03 relative to Lot 02 resulted from the annealing above T_g

that caused growth in the ice crystals. In contrast to the SSA value, there was no significant difference in the water content (0.10 ± 0.00 to 0.12 ± 0.01). Notably, the water content is the remaining water in the lyophilized Flomoxef. The residual water was sublimated from the Flomoxef. Therefore, the SSA value increased under the same water content, implying the generation of small ice in Lot 01 relative to Lot 03. An SEM observation was then performed to confirm the microscopic structure of the ice after lyophilization. The SEM image indicated the mass of Flomoxef after the lyophilization, strongly indicating the formation of micropore structures of Flomoxef via the sublimation of ice of a small size (Figure 7(a)).

The product temperature T_b was then monitored from the initial to the final freezing temperature (-41.5 °C). Figure 8 (a) shows the typical profile of the T_b value of Lot 03 during the freezing stage. The freezing temperature of the product is -3.3 °C. However, the further decrease in T_b to -10 °C or lower was observed after the T_b value reached -3.3 °C, which corresponded with the supercooling. Supercooling during the freezing stage to -10 °C or lower was observed in both vials at the center and edge in the lyophilizer. Following the freezing stage, annealing was performed such that the product temperature could be in a range between the freezing temperature and the glass-transition temperature.

Table 6 Results of SSA and Water Content for the Lyophilized Cakes (Lots 01 to 06)

	Quality attributes	
	SSA (m ² /g)	Water content (%)
Lot 01	0.64 ± 0.05	0.10 ± 0.00
Lot 02	0.50 ± 0.01	0.11 ± 0.04
Lot 03	0.40 ± 0.01	0.12 ± 0.01
Lot 04	0.14 ± 0.01	0.21 ± 0.04
Lot 05	0.10 ± 0.01	0.24 ± 0.00
Lot 06	0.04 ± 0.01	0.41 ± 0.03

Values shown are the average \pm standard deviation (S.D.) All the experiments were performed thrice. ## Lots 01–03 and Lots 04–06 were lyophilized in different manners.

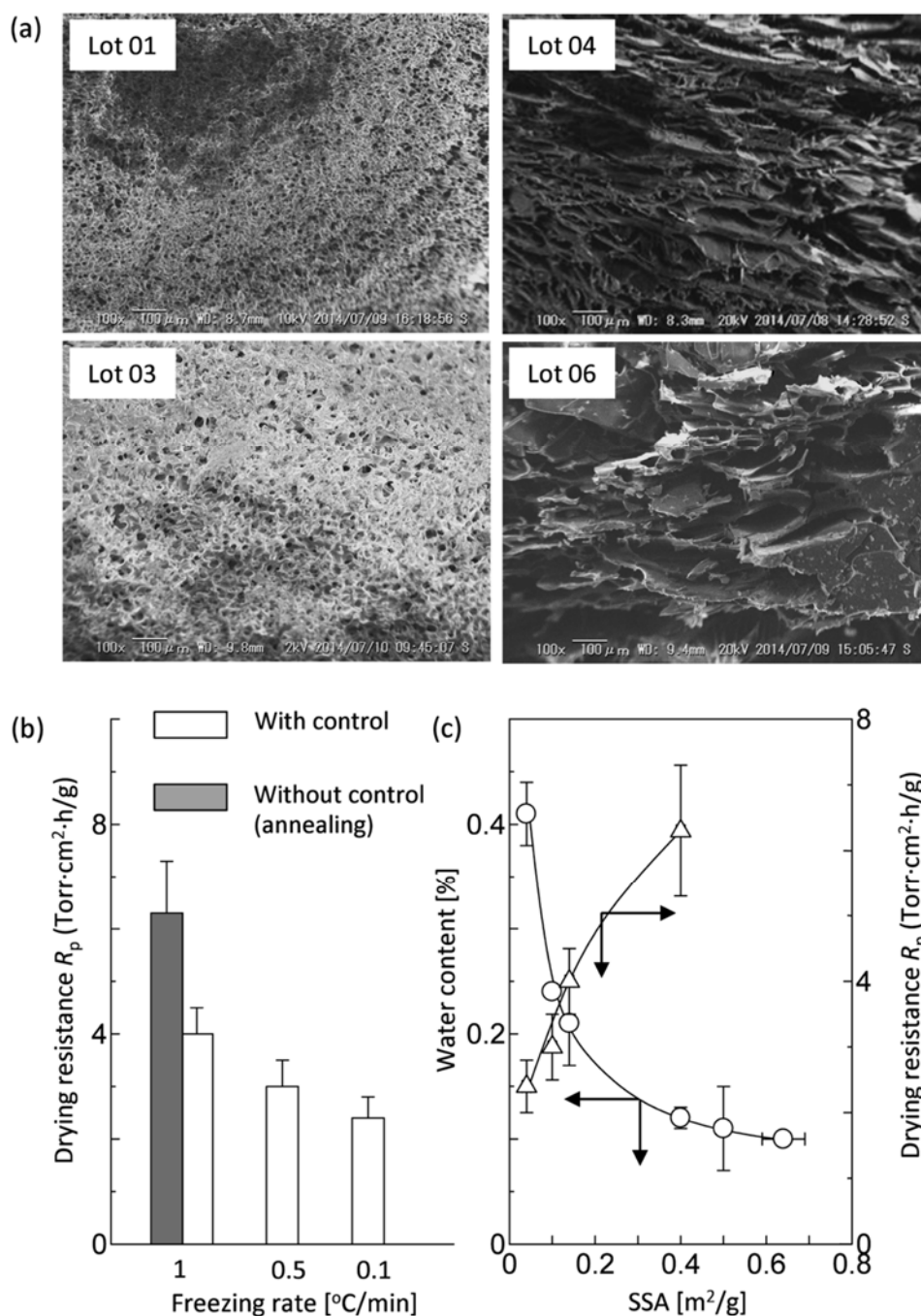


Figure 7 (a) SEM Images of Ice Crystals in Vials (Lots 01, 03, 04, and 06)

The details of experimental conditions for SEM images are summarized in Table 4. (b) Effect of the freezing rate on the drying resistance. (c) Water content and drying resistance as a function of the SSA of lyophilized cakes.

3.4.3 Lyophilization with a Temperature-Controlled Nucleation Step

After equilibration of the vials on the shelf at $-5\text{ }^{\circ}\text{C}$, the pressurization and depressurization of the chamber was conducted to control the ice nucleation. Figure 8 (b) shows the profile of the T_b value of Lot 04 during the freezing stage. Freezing at $5\text{ }^{\circ}\text{C}$ was observed in both vials placed at the center and edge of the lyophilizer after depressurization and supercooling was not found when the shelf temperature was reduced to $-41.5\text{ }^{\circ}\text{C}$. The difference between Lot 03 (Figure 3(a)) and Lot 04 (Figure 3(b)) was the addition of the pressurization and depressurization. It was, therefore, considered that the dissipation of supercooling might be a result of the addition of pressurization and depressurization. Moreover, the SEM image of Lot 4 indicated the formation of large micropores in the Flomoxef, as compared to the case of Lot 03. This result suggested the addition of the pressurization and depressurization induced the formation of large ice in the Flomoxef.

As another factor to control the size of ice, the freezing rate was maintained from $0.1\text{ }^{\circ}\text{C}/\text{min}$ to $1\text{ }^{\circ}\text{C}/\text{min}$ (Lots 04–06). Both the SSA value and water content of Lot 04 to Lot 06 were investigated (Table 3). The SSA value decreased from 0.14 ± 0.01 to 0.04 ± 0.01 . Moreover, the water content increased from 0.21 ± 0.04 to 0.41 ± 0.03 in accordance with the decreasing freezing rate. The ice of Lot 06 showed the smallest SSA value and the highest water content. In contrast, the ice of Lot 04 showed the opposite values, which decreased the water desorption rate during the secondary drying stage and led to increased residual water content. In addition, the cooling rate for Lot 06 was less than that for Lot 04. Therefore, the slower cooling rate was considered to cause growth of ice crystals. A comparison of SEM images between Lots 04 and 06 showed the coarsely pored structure of the ice crystals in Lot 06 as shown in Figure 7 (a), demonstrating the formation of large ice in the Flomoxef of Lot 06 relative to Lot 04. Thus, the control of ice size via the freezing rate can be termed ice

nucleation control.

Both the growth of ice crystals and their size should be related to the resistance of the water vapor to the frozen Flomoxef cake. Then, the average R_p value during the primary drying stage was calculated using Equation (9) as shown in Figure 7. The R_p value of Lots 04 to 06 decreased with a decrease in the freezing rate as shown in Figure 7 (b). This was because slower cooling was confirmed to cause growth of ice crystals as previously discussed. The R_p values with ice nucleation control became lower than those of the product (Lot 03) without any ice nucleation control (i.e., annealing). This demonstrated that the ice nucleation control contributed to a reduction in the drying resistance.

The water content of the products and their SSA are presented in Table 6 and again summarized in Figure 7c. The increase in the SSA value induced reduction in the water content and increase in the R_p value. The smaller ice crystals such as those of Lot 01 were disadvantageous for the sublimation of water. Meanwhile, the larger ice crystals appeared to induce rapid sublimation under low water vapor resistance. Therefore, the ice nucleation control enabled shortening of the primary drying time because of the formation of large ice in the Flomoxef.

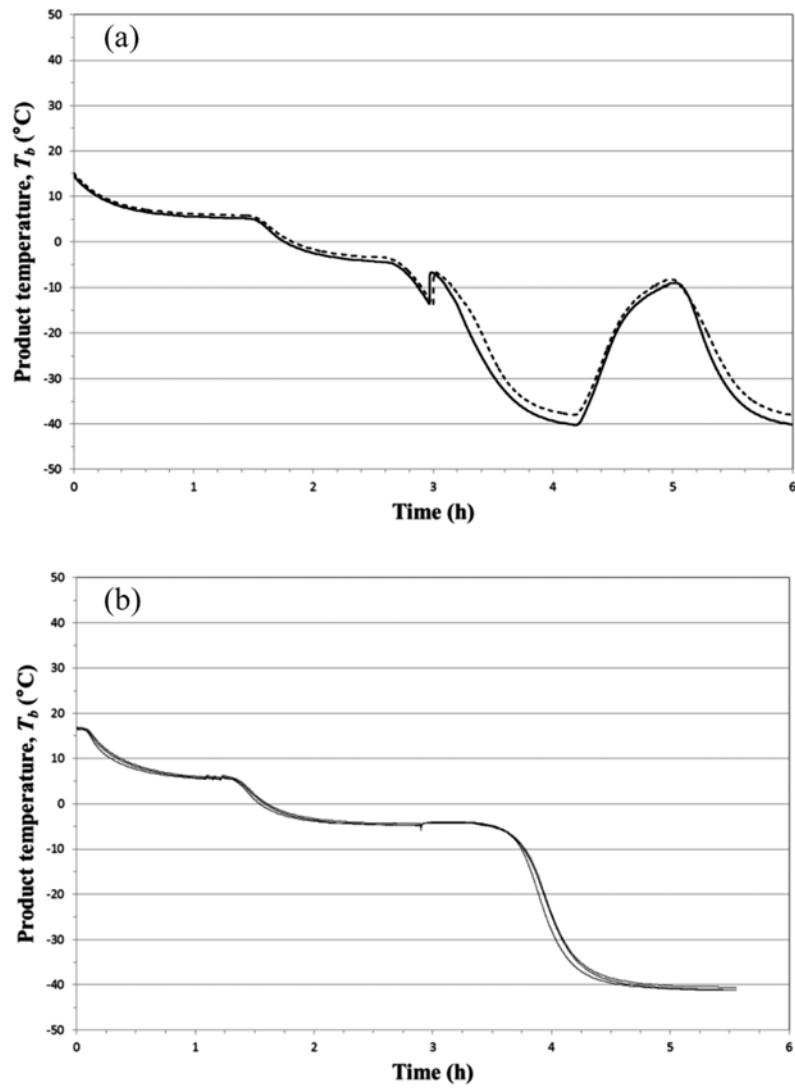


Figure 8 Product Temperature Profile during the Freezing Stage (a) without and (b) with Ice Nucleation Control

(a)Lots 03 and (b) 04 were used. Solid line: The vial placed at the center position in the lyophilizer; dotted line: the vial placed at the edge position in the lyophilizer.

Table 7 Average Resistance of the Dried Product Layer during Primary Drying Stage

Lot	Freezing Condition	Freezing Rate (°C/min)	Trial Number (<i>n</i>)	Water Vapor Transfer Resistance of the Dried Layer (R_p) (Torr·cm ² ·h/g) ^{a)}
Lot 03	Non-nucleation control Annealing: 0°C for 0.5 h	1	4	6.3 ± 1.0
Lot 04	Nucleation controlled at -5°C	1	3	4.0 ± 0.5
Lot 05	Nucleation controlled at -5°C	0.5	3	3.0 ± 0.5
Lot 06	Nucleation controlled at -5°C	0.1	3	2.4 ± 0.4

a) Average ± S.D. The values of the parameters to estimate R_p value are as follows: $W_{\text{fill}}=3.64$ g, $\rho_{\text{ice}}=0.918$ g/mL, $\rho=1.156$ g/mL, $C=0.31$ g/g, $A_p=3.84$ cm², $A_v=4.71$ cm², $L_{\text{max}}=0.73$ cm, $\Delta_{m\text{H}_2\text{O}}=2.51$ g/vial, $\Delta H=669$ cal/g, and $104 K_v$ (at 6.7 Pa)=2.57 cal/(s·cm²·°C).

3.4.4 Calculation of the Design Space for the Primary Drying Stage

The sublimation interface temperature during primary drying was established using the drying resistance ($R_p = 4.0$) with ice nucleation control and the drying resistance ($R_p = 6.3$) without ice nucleation control, as listed in Table 8. With ice nucleation control, when both the T_s and P_c values were designed at -10 °C and 6.7 Pa, respectively, it was predicted that the sublimation temperature of the vials placed at both the center and edge positions in the lyophilizer during the primary drying stage can be controlled at a temperature lower than the cake collapse temperature (T_c). In contrast, without ice nucleation control, the sublimation temperature of the vials placed at the center position in the lyophilizer can be controlled at a temperature lower than T_c but the sublimation temperature of the vials placed at the edge position in the lyophilizer was the previously calculated T_c . Operating conditions (chamber pressure and primary drying time) that result in the shelf temperature increase from -25 °C to

0 °C and those resulting in the product temperature increase from -33 °C to -26 °C are summarized in Figure 9. Because the product temperature during the primary drying should preferably be from 2 °C to 5 °C lower than the collapse temperature [13], the acceptable region of the product temperature would be from -33 °C to -30 °C considering the T_c of the Flomoxef sodium bulk solution which is -28 °C. As illustrated in Figure 9 (a) and (b), the product temperature with ice nucleation control during the primary drying stage was confirmed to be within the acceptable region. In contrast, as illustrated in Figure 9 (d), the product temperature without ice nucleation control in the edge position in the lyophilizer during the primary drying stage was confirmed to be outside the acceptable region, although the product temperature with ice nucleation control at the center position was within the acceptable region (Figure 9 (c)).

Table 8 Predicted Sublimation Interface Temperature and Primary Drying Time (Calculated Using the Drying Resistance) under Ice Nucleation Control under a Condition of a Shelf Temperature of -10°C and a Chamber Pressure of 6.7 Pa

Ice nucleation control	Drying resistance R_p (Torr·cm ² ·h/g)	Product temperature (T_b) (°C)	Sublimation interface temperature (T_{ice}) (°C)
With control	4.0	Center	-32.8
		Edge	-30.0
Without control	6.3	Center	-30.3
		Edge	-27.5

The values of the parameters to calculate R_p value are as follows: $W_{fill}=3.64$ g, $\rho_{ice}=0.918$ g/mL, $\rho=1.156$ g/mL, $C=0.31$ g/g, $A_p=3.84$ cm², $A_v=4.71$ cm², $L_{max}=0.73$ cm, $\Delta_{mH_2O}=2.51$ g/vial, $\Delta H=669$ cal/g, $10^4 K_v$ (center)=2.57 cal/(s·cm²·°C), and $10^4 K_v$ (edge)=4.11 cal/(s·cm²·°C). LyoStar 3 as a lyophilizer was used to estimate the K_v value.

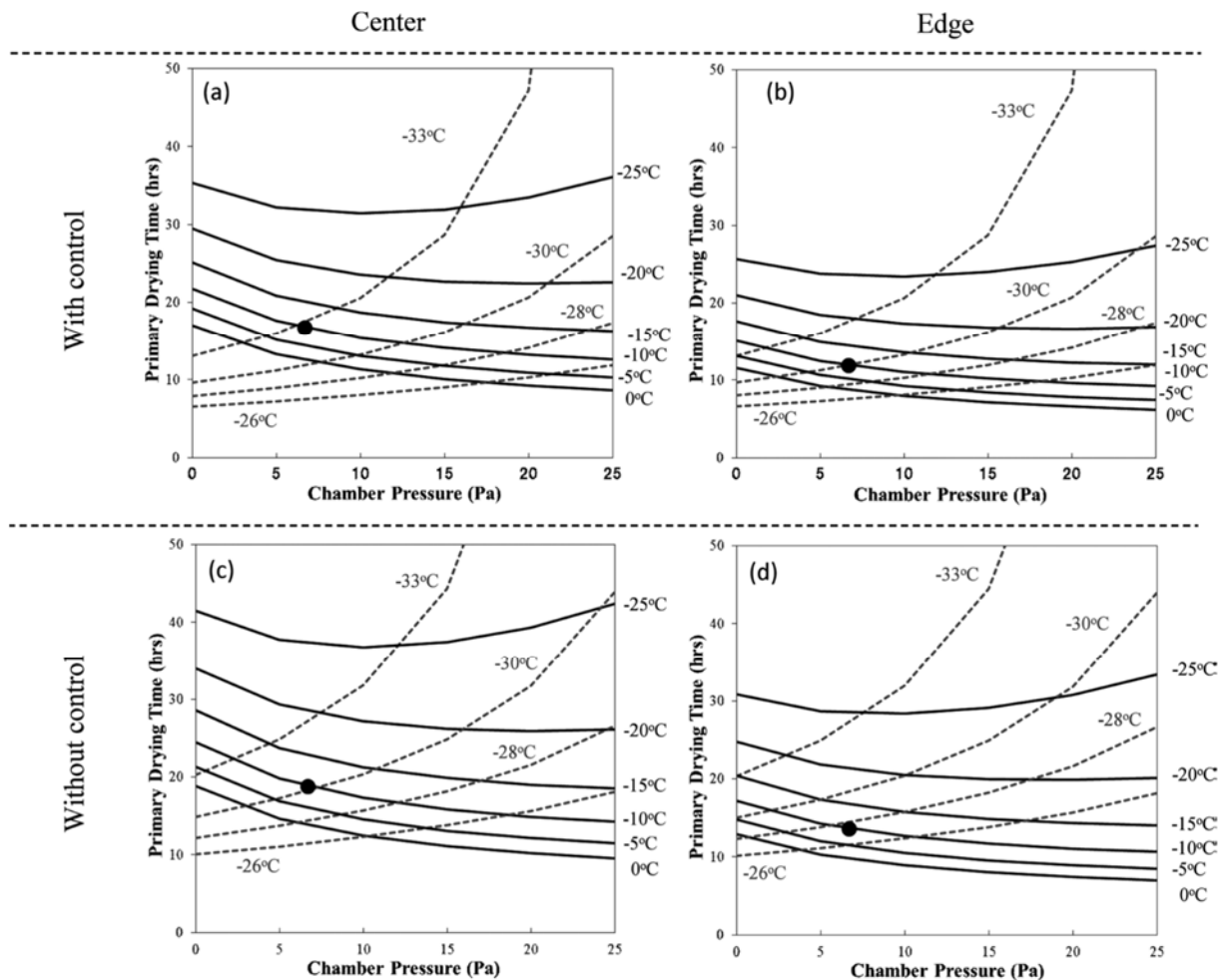


Figure 9 Design Space for the Primary Drying Stage with and without Ice Nucleation Control

Operating conditions with ice nucleation control ($R_p=4.0$) at the (a) center and (b) edge positions. Operating conditions without ice nucleation control ($R_p=6.3$) at the (c) center and (d) edge positions. Solid line: Operating conditions (chamber pressure and primary drying time) resulting in the same shelf temperature from -25 to 0°C . Dotted line: Operating conditions (chamber pressure and primary drying time) resulting in the same product temperature from -33 to -26°C . Closed circle: operating condition at -10°C for the shelf temperature and 6.7 Pa for the chamber pressure.

3.4.5 Verification Study for the Primary Drying Conditions Based on the Design Space

Two lots (Trials 01 and 02) of manufacturing were performed to verify the primary drying conditions calculated using the design space.

Trial 01 was manufactured with ice nucleation control and visual inspection was conducted for all 726 vials after the completion of the lyophilization. Consequently, there were *no collapsed cakes*. In contrast, Trial 02 was manufactured without ice nucleation control. As predicted in the previous design space, some collapsed cakes were observed in the vials placed at the edge position in the lyophilizer. The defective rate of the collapsed cake was 18%. It may be concluded that the R_p value of Trial 01 and the variation with ice nucleation control became lower than those of Trial 02, which was the product without ice nucleation control. The ice nucleation control enables a robust design space for the primary drying stage to be established with high productivity.

3.4 Conclusion

Our study demonstrated that the ice crystal size has an impact on the product quality and productivity. The pressurization and depressurization technique were combined by varying the freezing rate to avoid supercooling of the solution and control the size of the ice formed in the drug product during the freezing stage, which contributed to a reduction in R_p during the primary drying stage. This approach was termed ice nucleation control, which was advantageous in shortening the primary drying time. The reduced R_p made it possible to set the robust design space for the primary drying stage to achieve uniform products with higher productivity (no collapsed cakes in 726 vials).

Thus, our study emphasizes the impact of ice nucleation control on the quality and productivity of a small-molecule pharmaceutical product. However, the increase in the residual water content of the lyophilized cake may affect the solid stability. A stability test to determine the maximum allowable water content is needed, which will be the topic of our future investigation.

Chapter 4: Temperature Measurement by Sublimation Rate as a Process Analytical Technology Tool in Lyophilization

4.1 Introduction

The freezing step and secondary drying stage are typically completed within a few hours [13,20,21]. Conversely, the primary drying stage could take days or week if the process parameters are improper [6,7,8,9,22]. Therefore, an important issue for the industrial lyophilization process corresponds to shortening and optimizing the primary drying stage [50,51]. A critical issue in the lyophilization of drug products corresponds to excessive temperature elevation. During the primary drying stage, the product temperature (T_b) increases excessively and causes the collapse (improper freeze drying) of the product [26]. Cake collapse temperature (T_c) denotes the temperature above which the lyophilized product loses its macroscopic structure and the cake collapses during the primary drying process. In order to produce an acceptable lyophilized product, it is always necessary to perform primary drying at a temperature lower than T_c . Additionally, the primary drying stage generally corresponds to the longest stage in the lyophilization process. The costs are significantly reduced by optimizing and shortening the procedure. Therefore, important issues in the lyophilization field include the monitoring of T_b and determination of the end point of the primary drying stage.

With respect to the effective monitoring of T_b and the end point of the primary drying stage, various process analytical techniques (PAT) are developed in the field of lyophilization. A few scientific reports evaluated the advantages and disadvantages of the aforementioned techniques [52,53]. It is expected that the PAT clarifies knowledge on critical material attributes and their relationship with the manufacturing process. Therefore, PAT tools focused on critical material

attributes and critical process parameters. For examples, the T_b and water vapor transfer resistance of the dried layer (R_p) are well-known as critical material attributes. The shelf temperature (T_s), chamber pressure (P_{dc}), and drying time are used as critical process parameters. Thus, PAT tools are developed to monitor the aforementioned targets mentioned. Specifically, PAT is categorized into techniques for a single vial and batch operation as shown in Table 9.

A wire thermocouple (TC), resistance thermal detectors (RTD), temperature remote interrogation system (TEMPRIS) are well-known as PAT tools for a single vial. The TC is used to monitor the T_b value in laboratory scale lyophilizer. It is difficult to adjust TCs at the center bottom position in the vials, [53], and this is causes intra- and inter-batch variations in the T_b -profile [54]. Additionally, the T_b -profile mapping in the pilot or production lyophilizer is typically not available because the TCs are not available or interfere with automatic loading systems. This results in a low accuracy in terms of determining the end pint of the primary drying. In order to solve the aforementioned problems, TEMPRIS as a wireless temperature sensor is proposed as an effective means. Specifically, TEMPRIS is always available to be adjusted at the center bottom in the vials, and therefore narrow variations in the T_b -profile for intra- and inter-batch are expected. Moreover, it is expected that the end point of primary drying will be accurately monitored. Furthermore, the possibility of using the same sensors in the laboratory, pilot and production lyophilizer aids in easily and rapidly performing scale-up experiments. A previous study examined the TEMPRIS system for application in freeze drying [54]. In the development phase of lyophilization cycle, a single vial monitoring as a PAT tool is useful since it is necessary to understand the T_b -profile mapping including the difference in the temperature profile of the vials placed at center and edge position in the lyophilizer to optimize the lyophilization cycle. As discussed above, TEMPRIS is an important PAT method to monitor

a single vial. Furthermore, a scalable application of TEMPRIS continues to be vital.

Batch monitoring as a PAT method is effective in monitoring the designed lyophilization cycle, deepening the cycle, and performing a continuous cycle improvement. The PAT tools for the batch system are shown in Table 9. The Pirani gauge works on the principle of measuring the thermal conductivity of the gas in the drying chamber [55]. The Pirani gauge is typically calibrated by nitrogen gas and reads approximately 60% higher than a capacitance manometer during the primary drying stage since almost all the gas in the chamber corresponds to water vapor [56]. This is because the thermal conductivity of water vapor is approximately 1.6 times that of nitrogen [56]. When a lyophilizer with a nitrogen leak system is used, the gas composition in the chamber changes from water vapor to nitrogen at the end of primary drying since sublimation is completed and nitrogen gas leaks into the chamber to control the chamber pressure. Pirani is dependent on the gas composition in the chamber [55], and the Pirani pressure indicates the primary drying endpoint with a sharper pressure decrease towards the capacitance manometer pressure. It is reported that Pirani gauge withstands steam sterilization [56], and thus utilization of the Pirani pressure monitoring is an effective means to determine the end point of the primary drying stage during the early phase of lyophilization cycle development and also the application of Pirani pressure monitoring to commercial production since a PAT tool is useful in cycle verification and continuous improvement. A mass spectrometer is a candidate PAT tool to determine the end point of primary drying and secondary drying. A few potential applications for pharmaceutical lyophilization are reported [57]. Tunable diode laser absorption spectroscopy (TDLAS) is well-established at the laboratory scale and directly measures the water vapor concentration in the duct connecting the chamber and condenser [56,58,59]. Specifically, TDLAS is an expensive technique that is not a standard accessory with a lyophilizer. The evaluation of manometric temperature

measure (MTM) is a well-known technology to monitor the primary drying stage [37,38,49]. The featured point in MTM corresponds to a laboratory scale technology to measure the T_b via isolating the valve between the chamber and condenser within approximately 30 s. The resulting pressure-rise in the drying chamber yields the sublimation interface temperature (T_{ice}) and R_p . However, the application of MTM to a production lyophilizer is challenging. This is because most production scale lyophilizers do not allow the isolation of the valve between the chamber and condenser within 30 s. Additionally, at the end of the primary drying, there is no or little pressure increase because the sublimation of ice is completed. The calculated value for vapor pressure of ice corresponds to P_{dc} , and the calculated T_{ice} rapidly decreases. Thus, it is not possible to monitor the T_b variation during the later stage of primary drying and the period of transition from primary drying to secondary drying. Therefore, TDLAS and MTM experience difficulties in terms of their scalable application to the lyophilizer.

Recently, a monitoring system without valve operation is proposed by using a laboratory scale lyophilizer, and this is termed as the valveless monitoring system (VMS) [60]. The VMS monitors the sublimation rate in a noninvasive manner and yields the vial heat transfer coefficient (K_v) as well as R_p , and T_b values. Based on the aforementioned outcomes, VMS-based calculation of the design space for a specific product is demonstrated. The VMS algorithm used an equivalent length that accounts for pressure loss due to the straight pipe, valves, fittings, bends in the pipe, and entrance/exit effects. Thus, a VMS algorithm is in principle applicable to laboratory scale lyophilization and also to production scale lyophilization. Furthermore, VMS is limited to the laboratory scale [61]. A scalable application of VMS is promising in terms of obtaining more reliable and comparable process information.

In the present study, it is proposed that the resistance coefficient can aid in expressing the pressure drop along the main pipe of lyophilization and is an alternative to the equivalent length.

The approach yields the resistance coefficient of the path along the main pipe of the lyophilization even in the case in which its equivalent length is unknown such as the scale-up. Furthermore, we also considered the algorithm that does not require the estimation of K_v value. We propose a novel measurement system by considering the difference in specification of lyophilizers as the temperature measurement by sublimation rate (TMbySR) system [62] for the same year as the first report [60] with respect to VMS. The study discusses the potential use of TMbySR system as a PAT method. First, the rate of sublimation was elucidated based on the viscous flow of vapor in the lyophilization. The key parameter corresponded to the resistance coefficient that accounted for the pressure drop along the main pipe. Next, the sublimation rate was converted to T_b . The measurement of the endpoint of the primary drying stage was attempted from the obtained T_b -profile. The plausibility of TMbySR was examined from the verification test of the product quality and the comparison with TEMPRIS.

Table 9 Process Analytical Technology (PAT) Methods in the Lyophilization

Target	PAT method	Measurement parameter	Ref.
Single vial	TC	T_b	54
	RTD	T_b	54
	TEMPRIS	T_b	54
Batch	Pirani vs Capacitance manometer	P_{dc}	55,56
	Mass spectrometer	Partial pressure of gas	57
	TDLAS	Water vapor concentration	56,58,59
	MTM	T_b	37,38,49,56
	VMS	T_b	60,61
	TMbySR	T_b	This study

*TC: Wire thermocouple, RTD: Resistance thermal detectors, TEMPRIS: Temperature Remote Interrogation System, TDLAS: Tunable diode laser absorption spectroscopy, MTM: Manometric Temperature Measurement, VMS: Valveless Monitoring Method, TMbySR: Temperature Measurement by Sublimation Rate

4.2 Experimental

4.2.1 Materials

Flomoxef sodium solution for injection (molecular weight: 518.45, CAS No. 92823-03-5) including sodium chloride as the stabilizing agent was prepared with WFI. The total solid content of the solution corresponded to 31% (w/w, liquid density: 1.156 g/mL). Specifically, 14-mL vials manufactured from clear, colorless, and round borosilicate glass tubing that satisfy the USP criteria for Type I glass, and stoppers suitable for the lyophilization that are manufactured from chlorinated butyl elastomer were used in the investigation. The freezing temperature of Flomoxef sodium solution and its glass-transition temperature correspond to $-3.3\text{ }^{\circ}\text{C}$ and $-31\text{ }^{\circ}\text{C}$, respectively [50].

4.2.2 TMbySR Algorithm

The sublimation rate is calculated from the measured data of the chamber pressure P_{dc} , condenser pressure P_{ct} , and shelf temperature T_s . The average product temperature at the center bottom of the vial T_b is previously computed, and the sublimation interface temperature T_{ice} is then calculated from the heat transfer coefficient of ice.

(1) Evaluation of sublimation rate

The sublimation rate Q_m (kg/h) is computed from the chamber pressure P_{dc} (Pa) and condenser pressure P_{ct} (Pa) that are measured by two capacitance manometers installed in the

drying chamber and condenser of the lyophilizer, respectively. The water vapor sublimated from the sublimation interface of the dried material flows into the condenser through the main pipe from the drying chamber and is trapped on the coil of the condenser. The flow of vapor through the main pipe is considered as a viscous flow with leak type pressure control, and thus the Q_m value from the dried material is calculated via the pressure difference between the chamber and condenser (ΔP) as follows:

$$Q_m = \frac{3.6(P_{dc} - P_{ct})}{R_a} = \frac{3.6\Delta P}{R_a} \quad 4 - (1)$$

where R_a (kPa s/kg) denotes the water vapor transfer resistance through the main pipe. A value of 3.6 (= 3600/1000) is obtained for the unit conversion of time (h and s) and pressure (Pa and kPa). As indicated by a previous study, R_a includes the dried layer of product, semi-stoppered vial, and chamber per vial [33].

As expressed in equation (1), the rate of sublimation is determined by R_a . Specifically, the flow of vapor between the drying chamber and condenser chamber determines the rate of sublimation (see Fig.1). From the formula for the pressure drop along the pipeline, the pressure difference ΔP of a viscous flow with ρ (kg/m³) in vapor density corresponds to the product of kinetic energy of viscous flow with the water vapor transfer resistance coefficient through the main pipe C_r . The diameter and length of main pipe in the present lyophilizer are 158 mm and 562 mm, respectively (see Fig.1). Furthermore, ρ (kg/m³) is expressed via the state equation of ideal gas, $\rho = PM / (RT)$ (P : vapor pressure (Pa); M : molecular weight (g/mol), R : gas constant (J/(K kmol)), T : vapor temperature (K)), u denotes the flow rate (m/s), A denotes the flow passage area of the main pipe (m²). Therefore, the pressure difference ΔP is described as

follows:

$$\Delta P = C_r \times \frac{1}{2} \rho u^2 = \frac{1}{2} C_r \rho \left(\frac{Q_m}{3600 A \rho} \right)^2 \quad 4 - (2)$$

Under the assumption that the water vapor corresponds to the ideal gas, and the molecular weight $M = 18$, gas constant $R = 8314$, and gas temperature $T = 288$ are substituted into equations (1) and (2) to obtain equation (3) as follows:.

$$Q_m = A \left(\frac{P_{dc}^2 - P_{ct}^2}{8314 \times 288 \times C_r / (18 \times 3600^2)} \right)^{1/2} = A \left(\frac{P_{dc}^2 - P_{ct}^2}{0.0103 C_r} \right)^{1/2} \quad 4 - (3)$$

The use of equation (3) is useful because the estimation of R_a value in equation (1) is not required. Alternatively, it is necessary to evaluate the C_r for each lyophilizer via the water sublimation test because there are differences in the state of main pipe and valves for each lyophilizer. When the resistance values are obtained, the values are used as the control constant for each lyophilizer.

(2) Evaluation of average product temperature at the center bottom of the vial

The average product temperature at the center bottom of the vial, T_b , of the batch during the primary drying stage and transition stage to secondary drying from primary drying is computed from the following equations.

First, the heat input Q_g from the shelf to the bottom of all vials via gas conduction is calculated as follows:

$$Q_g = K_g A_e (T_s - T_b) \quad 4 - (4)$$

where A_e denotes the effective heat transfer area (m^2), K_g denotes the heat transfer coefficient from the shelf to the vial bottom via gas conduction ($\text{W}/\text{m}^2 \text{K}$), T_s denotes the shelf temperature, and T_b denotes the average product temperature at the center bottom of the vial (K).

The heat transfer coefficient from the shelf to the vial bottom via gas conduction K_g ($\text{W}/\text{m}^2 \text{K}$) is described as follows:

$$K_g = \frac{\lambda}{\delta + L} = \frac{\lambda}{\delta + \frac{\lambda}{\Lambda P_{dc}}} = \frac{16.86}{\delta + 2.2 \times 29 \times 0.133/P_{dc}} \quad 4 - (5)$$

where λ denotes the thermal conductivity of water vapor and corresponds to 0.0168 ($\text{W}/\text{m K}$), δ is the average distance between vials bottom and the shelf (mm), and mean free length L (m) is expressed as $(\lambda/\Lambda P_{dc})/2.2 = 0.029/P_{dc}$ (mTorr). Hence, L (mm) is calculated as $29 \times 0.133/(P_{dc} \text{ (Pa)})$.

The effective heat transfer area A_e is calculated as $A_e = 2 / (1/A_v + 1/A_t)$, where A_v denotes the surface area of the outside diameter of the vial (m^2), and A_t denotes the tray frame area (m^2). Specifically, A_v is calculated as $A_v = \pi n_1 d^2 / 4$ (n_1 : vial number, d : outside diameter of the vial), and the tray frame area A_t is calculated as $A_t = n_2 W L$ (n_2 : frame number; W : width size of a frame, L : length size of a frame).

The radiation heat input Q_r from a drying chamber wall to all vials is calculated as follows:

$$Q_r = 5.67 \times 10^{-8} \varepsilon A_e (T_w^4 - T_b^4) = 5.67 \varepsilon A_e \left[\left(\frac{T_w}{100} \right)^4 - \left(\frac{T_b}{100} \right)^4 \right] \quad 4 - (6)$$

where ε denotes a radiation coefficient, T_w denotes the drying chamber wall temperature (K), and 5.67×10^{-8} denotes the Stefan-Boltzmann constant ($\text{W}/\text{m}^2 \text{K}^4$).

Furthermore, the radiation heat input Q_r from the drying chamber wall to all vials is described approximately as follows:

$$Q_r = K_r A_e (T_w - T_b) \quad 4 - (7)$$

where, K_r denotes a considerable heat transfer coefficient by radiation heat input, and it is approximated as $K_r = 0.7$ ($\text{W} / \text{m}^2 \text{ } ^\circ\text{C}$) with a laboratory scale lyophilizer (Trio-A04, total shelf of 0.4 m^2 , KYOWAC), and it is approximated as $K_r = 0.2$ ($\text{W} / \text{m}^2 \text{ K}$) with a production freeze dryer (RL-4536BS, total shelf area of 36.1 m^2 , KYOWAC).

Furthermore, heat Q_l required for the increase in temperature of the dried material and vials is calculated as follows:

$$Q_l = C_p \frac{dT_b}{dt} \quad 4 - (8)$$

where, C_p denotes the total calorific capacity of the dried material, vials, and rubber stopper (J/K).

From the relation between the heat input and sublimation latent heat $\Delta H_s = 2850$ (kJ / kg), we obtain the following equation:

$$\frac{Q_m \Delta H_s}{3600} + Q_l = Q_g + Q_r$$

$$\frac{Q_m \Delta H_s}{3600} + C_p \frac{dT_b}{dt} = K_g A_e (T_s - T_b) + K_r A_e (T_w - T_b) \quad 4 - (9)$$

where T_{b0} denotes the initial value of the product temperature at the center bottom of the vial in the primary drying, and Δt denotes the primary drying time. The average product temperature at the center bottom of the vial for the batch is calculated as follows:

$$T_b = \frac{K_g T_s + K_r T_w + \frac{C_p T_{b0}}{A_e \Delta t} - \frac{Q_m \Delta H_s}{3600 A_e}}{K_g + K_r + \frac{C_p}{A_e \Delta t}} \quad 4 - (10)$$

(3) Evaluation of average sublimation interface temperature

If the Q_m and T_b values are computed, the average sublimation interface temperature (T_{ice}) value is calculated from the equation of heat conduction of a frozen layer.

The heat transfer from the vial bottom to the sublimation interface Q_h is calculated via heat conduction of the frozen layer as follows:

$$Q_h = K_{ice} A_p \frac{T_b - T_{ice}}{L_{ice}} \quad 4 - (11)$$

where A_p denotes the surface area of the inside diameter of the vial (m^2), and K_{ice} denotes the heat transfer coefficient of ice ($W/(m^2 K)$), and L_{ice} denotes the thickness of the frozen layer (m).

Furthermore, the relationship between the heat transfer Q_h and Q_m value is described as follows:

$$Q_h = \Delta H_s Q_m \quad 4 - (12)$$

From equations (11) and (12), the average sublimation interface temperature T_{ice} is calculated as follows:

$$T_{ice} = T_b - \frac{\Delta H_s Q_m K_{ice}}{A_p L_{ice}} \quad 4 - (13)$$

4.2.3 Programmable Logic Controller (PLC) in Lyophilizer

Figure 10 shows the device configuration of the lyophilizer. Subsequently, PLC is memorized via the sequencer in the lyophilizer to compute the following quantities: (i) Q_m based on equation (3); (ii) T_b based on equation (10); and (iii) T_{ice} based on equation (13).

The accuracy of capacitance manometers is critical in measuring the pressure difference between the chamber and condenser (ΔP). They confirm the output linearity and are calibrated on a regular basis. Additionally, zero point adjustment is performed when they are installed in the chamber and condenser. Furthermore, the software for adjusting the output value of capacitance manometer in the condenser to that of the capacitance manometer in the dry chamber prior to the initiation of primary drying is installed in the PLC to accurately measure the ΔP during the primary drying step.

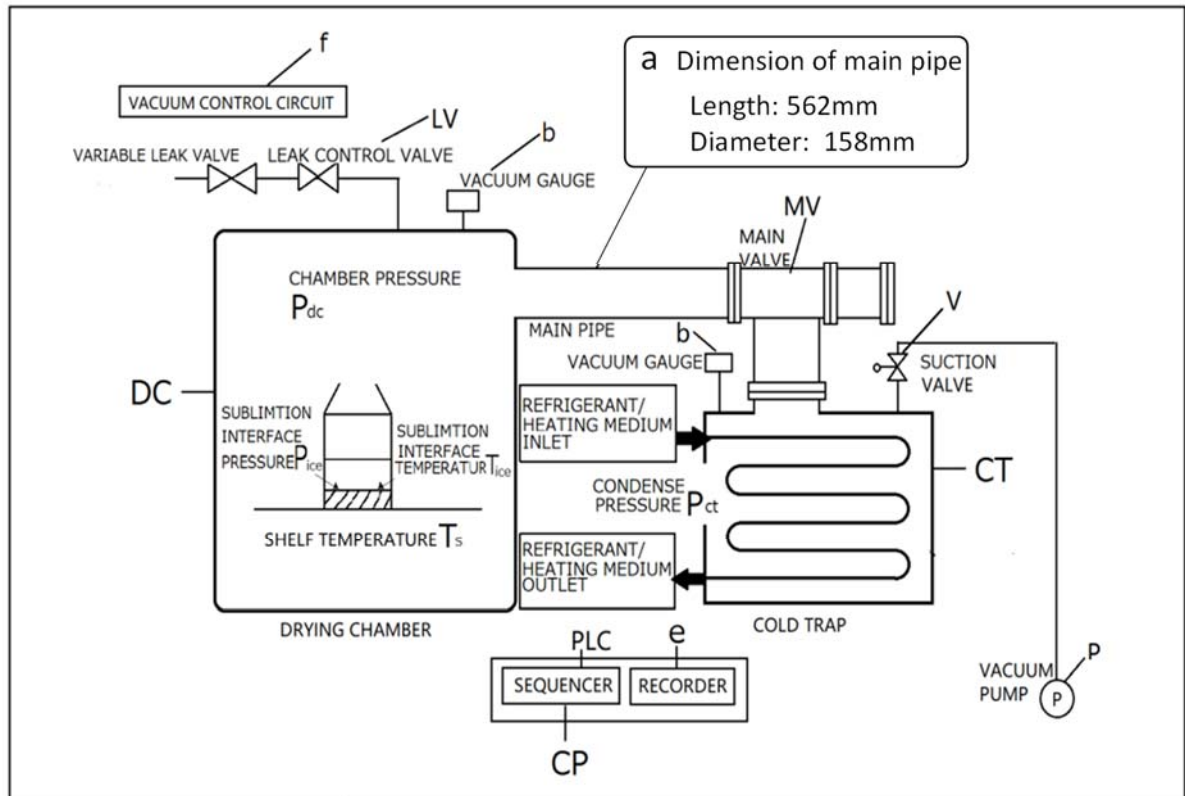


Figure 10 Device Configuration of the Lyophilizer.

DC: drying chamber, CT: cold trap, CP: control panel, LV: leak control valve, MV: main valve, PLC: programmable logic controller based on equations (3), (10) and (13), P: vacuum pump, V: suction valve, a: main pipe, b: vacuum gauge (capacitance manometer), e: recorder, f: vacuum control circuit.

4.2.4 Water Sublimation Test for Evaluating C_r

A water sublimation test was conducted to obtain the relationship between the C_r and Q_m values. A Lyophilizer Trio-A04 (total shelf area of 0.4 m^2 , KYOWAC) was utilized for the investigation. There are three shelves in the lyophilizer and one to three stainless steel trays filled with 500mL water for injection were loaded into the drying chamber. The freezing procedure was performed at $-47.5 \text{ }^\circ\text{C}$, and the primary drying conditions were designed at $-10 \text{ }^\circ\text{C}$ and $0 \text{ }^\circ\text{C}$ under the following two pressure conditions: 6.7 Pa and 10 Pa for 3 h. The mass after the lyophilization was measured, and the amount of water used for sublimation was

determined. The Q_m value was determined from the mass decrease in water associated with the sublimation for the first 3 hours (Δm) by using $Q_m = \Delta m/3$ (kg/h). The T_s , T_b , P_{dc} , and P_{ct} values were recorded over the lyophilization. It should be noted that the tray bottom part was measured as T_b . The C_r value was calculated from equation (3) by using the aforementioned data.

4.2.5 Case Study

Lyophilizer Trio-A04 equipped with TMbySR system (see Fig.10) was utilized in the experiments. Two lots (Lots 01 and 02) of manufacturing were performed to evaluate the measurement accuracy of the product temperature profile and ability to determine the end point of primary drying. The drying chamber of Lyophilizer Trio-A04 consists of three shelves and 220 vials of a 14-mL vial are completely placed on a shelf in the lyophilizer. Lots 01 and 02 were manufactured at the scales corresponding to 220 vials and 440 vials, respectively. Prior to the lyophilization of each lot, Flomoxef sodium bulk solution was filtered through a 0.2 μm filter. Specifically, 3.15 mL of the filtered Flomoxef sodium bulk solution was filled in the 14 mL vials. After filling, the vials were semi-stoppered and loaded into the lyophilizer. Each lot of Flomoxef sodium bulk solution was cooled to 5 °C for 1 h and then cooled to -5 °C for 1 h without ice formation. After the completion of pre-cooling, the shelf temperature was decreased to -41.5 °C at 1 °C/min and maintained for 2 h. It is then annealed at 0 °C for 0.5 h to control the product temperature below the freezing temperature that corresponds to -3.3 °C. The primary drying and secondary drying were performed at -10 °C under 6.7 Pa pressure and at 50 °C under 2 Pa pressure, respectively. The product temperature profile and end point of the primary drying of Lot 01 and 02 as determined by TMbySR system were compared to the measurement results of TCs [54] and comparative pressure [55,56].

4.2.6 Verification Test

Lyophilizer Trio-A04 equipped with TMbySR system was utilized for the experiments. Lot 03 was manufactured at 660 vials that correspond to the maximum scale in the lyophilizer. Manufacturing conditions including lyophilization cycles with the exception of the primary drying time are identical to those of Lot 01 and 02. The lyophilization stage was advanced to the secondary drying stage. The product temperature profile and end point of the primary drying as determined by TMbySR system were compared to the measurement results of TEMPRIS sensors (IQ Mobil Solutions GmbH) [54] and comparative pressure [55,56].

4.2.7 Other Experiments

A visual inspection was performed for all the 220, 440, and 660 vials after the lyophilization process. The water content of the lyophilized cakes is determined via the Karl Fischer (Kyoto Electronics Manufacturing, MKS-510N) coulometric titration method.

4.3 Result and Discussion

4.3.1 Water Vapor Transfer Resistance Coefficient through Main Pipe

In order to operate the lyophilizer based on the principle of TMbySR (i.e. PLC), the unknown parameter only corresponds to C_r . The C_r value was estimated via the sublimation test. The chamber pressure P_{dc} was designed as 6.7 and 10 Pa at $T_s = 0$ °C and -10 °C, respectively. The variation in the amount of filled water for 3 hours was measured to estimate the Q_m value. The P_{dc} , P_{ct} and Q_m values that were experimentally recorded were summarized in Table 12. The C_r values that were experimentally determined by equation (3) were also listed in Table 12.

It was likely that the measured C_r value decreased with increases in Q_m value. In order to construct the PLC for lyophilization process, the relationship between C_r and Q_m is required. The C_r values were then plotted relative to the corresponding Q_m value in Figure 11. From the graph, a regression between C_r and Q_m yielded the following relation: $C_r = 2.39 Q_m^{-1.09}$ with high correlation coefficient ($r^2 = 0.9991$) in the range of Q_m exceeding 0.0312 kg/h. This was comparable with the report that the minimum value of Q_m precisely measured with VMS corresponded to 0.03 kg/h [60]. The C_r value calculated from the regressed curve is then compared with the measured C_r value as shown in Table 2. A good agreement between both was observed within several percentages in relative error. Therefore, the substitution of the relation into Equation (3) yields the formula for Q_m as given in Equation (14).

$$Q_m = 0.46 A (P_{dc}^2 - P_{ct}^2)^{1.125} \quad 4 - (14)$$

where A denotes the flow passage area of the main pipe and corresponds to 0.018146 (m²) in the case of lyophilizer Trio-A04.

In the present lyophilization condition (up to 660-vial scale), the Q_m value was considered as ranging up to 100 kg/hr. Therefore, a scalable application of the above equation is possible. Thus, the equation (14) was updated again in the PLC of the lyophilizer.

Table 10 Results of the Water Sublimation Test to Determine Water Vapor Transfer Resistance through the Main Pipe (C_r) of the Lyophilizer

Water Loading Amount (g)	Shelf Temperature T_s (°C)	Chamber pressure P_{dc} (Pa)	Condenser pressure P_{ct} (Pa)	Sublimation rate Q_m (kg/h)	Water vapor transfer resistance coefficient of the main pipe C_r (-)	
					Measured value	Calculated value
					1000.9	-10
1002.9	-10	6.68	6.44	0.0314	102.00	103.93
1510	-10	6.68	6.21	0.0623	49.85	49.25
501.5	-10	6.69	6.00	0.0940	31.65	31.45
1514.3	0	9.99	9.36	0.1363	20.96	20.98

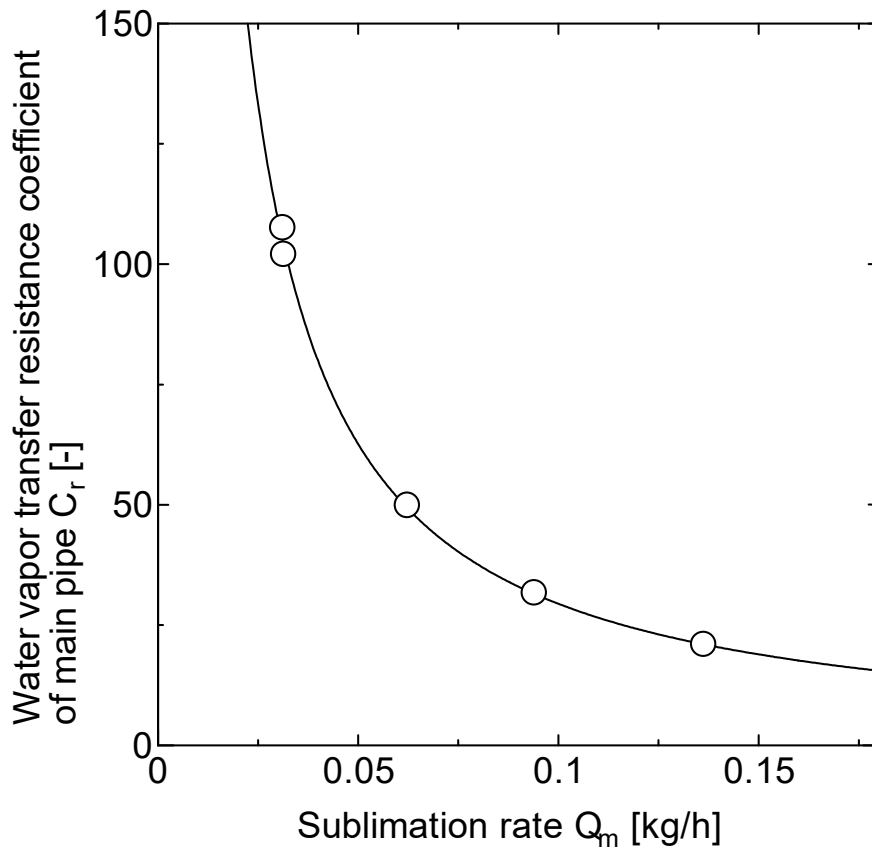


Figure 11 Relationship between the Sublimation Rate (Q_m) and Water Vapor Transfer Resistance Coefficient through the Main Pipe (C_r).

Solid curves represent the regressed curve. Correlation coefficient corresponds to 0.9991.

4.3.2 Monitoring of the Product Temperature Profile at 220- and 440-Vial Scales

4.3.2.1 220-Vial Scale

Initially, we checked the possibility of monitoring the primary drying stage with TMbySR. Here, the TC for monitoring a single vial was used as a comparison. Figure 12 (a) illustrates the temperature profile during the primary drying stage for Lot 01 of the Flomoxef sodium bulk solution (220 vials scale) monitored via the TC and TMbySR system. Additionally, the sublimation rate Q_m data obtained by TMbySR system was recorded to compare it with comparative pressure.

Prior to the comparison of TMbySR with TC, the vial position-specific outcome of TC

was initially discussed. Each TC used was positioned at the center bottom in the vials. This is because ice sublimation proceeds from the top to the bottom in the vials. It was expected that the last spot within the dried material where a remainder of ice was observed in the center bottom of the vial. Furthermore, the temperature profile of vials placed at the center and edge positions in the lyophilizer were compared with each other. Vials placed at the center position represented the longest steady state ice sublimation, and this was followed by a sharp increase step to the T_s after 20 h and essentially equilibrated to the T_s after 24 h. Conversely, vials placed at the edge position in the lyophilizer exhibited shorter steady ice sublimation, and this was followed by a sharp increase step after 10 h and 12.5 h. The drying process of edge vials significantly depended on receiving the radiation heat effect from the wall and additional heat from the surrounding vials that were already dried. The overheated state of vials (approximately -6°C) at the later phase of the primary drying stage was also due to the aforementioned reason. The comparison indicated that a deviation in the T_b -profile between two vials placed at the edge was evidently not negligible relative to that of vials placed at the center position. Thus, it was considered that the data of TCs loaded into vials placed at the center position in the lyophilization was available to compare it with TMbySR.

Next, we discuss monitoring using TMbySR. The sublimation rate Q_m of Lot 01 obtained by TMbySR system was displayed as blue-colored solid curves. The Q_m value at the steady state was approximately 30×10^{-3} (kg/h), and this was shown in the calibration curve in Fig.11. The Q_m was then converted to the T_b - and T_{ice} -profiles via equations (10) and (13) as shown in the red-colored closed and open circles, respectively in Figure 3(a). The T_b -profile was slightly higher than the T_{ice} -profile in the early primary drying stage. This was because the thickness of frozen layer to be sublimated was higher and because the temperature difference between the sublimation interface and vial bottom increased at the early primary drying stage. Conversely,

the T_b and T_{ice} at the late primary drying stage were almost identical. This was because the thickness of frozen layer was lower and the temperature difference between the sublimation interface and vial bottom reduced in the late primary drying stage.

The T_b obtained by TMbySR system corresponded to an intermediate temperature between the TCs temperature placed at the center and edge position in the lyophilizer at steady state ice sublimation, and this was followed by an increase to T_s after 12.5 h and equilibration at T_s after 24 h. The essential equilibration time to the T_s obtained via the TMbySR temperature reading exhibited excellent agreement with the TCs loaded to the vials placed at the center position in the lyophilizer.

The generally accepted definition of the end point for the primary drying while using TCs corresponds to when the temperature reading of the sensor is essentially equivalent to the shelf temperature (offset) or when the temperature reading exceeds the shelf temperature [63]. The T_b increased at approximately 12.5 h, and its equivalent time to the T_s corresponded to 24 h. The midpoint corresponding to the half of incremental change was 17.5 h for TMbySR. Conversely, pirani pressure ($P_{ac}(pir)$) indicated a primary drying endpoint with a sharper pressure decrease towards the capacitance manometer pressure ($P_{ac}(cm)$) after 21 h (Figure 12(b)). The TMbySR exhibited slightly better agreement with the primary drying endpoints as indicated via the TCs as opposed to the comparative pressure. The temperature profile obtained by TMbySR system indicated the representative temperature profile of the batch. The end point of the primary drying determined by TMbySR temperature reading was in agreement with the end point detected via the TCs. Specifically, 220 lyophilized vials of Lot 01 were visually inspected, and there was no cake collapse as shown in Table 11.

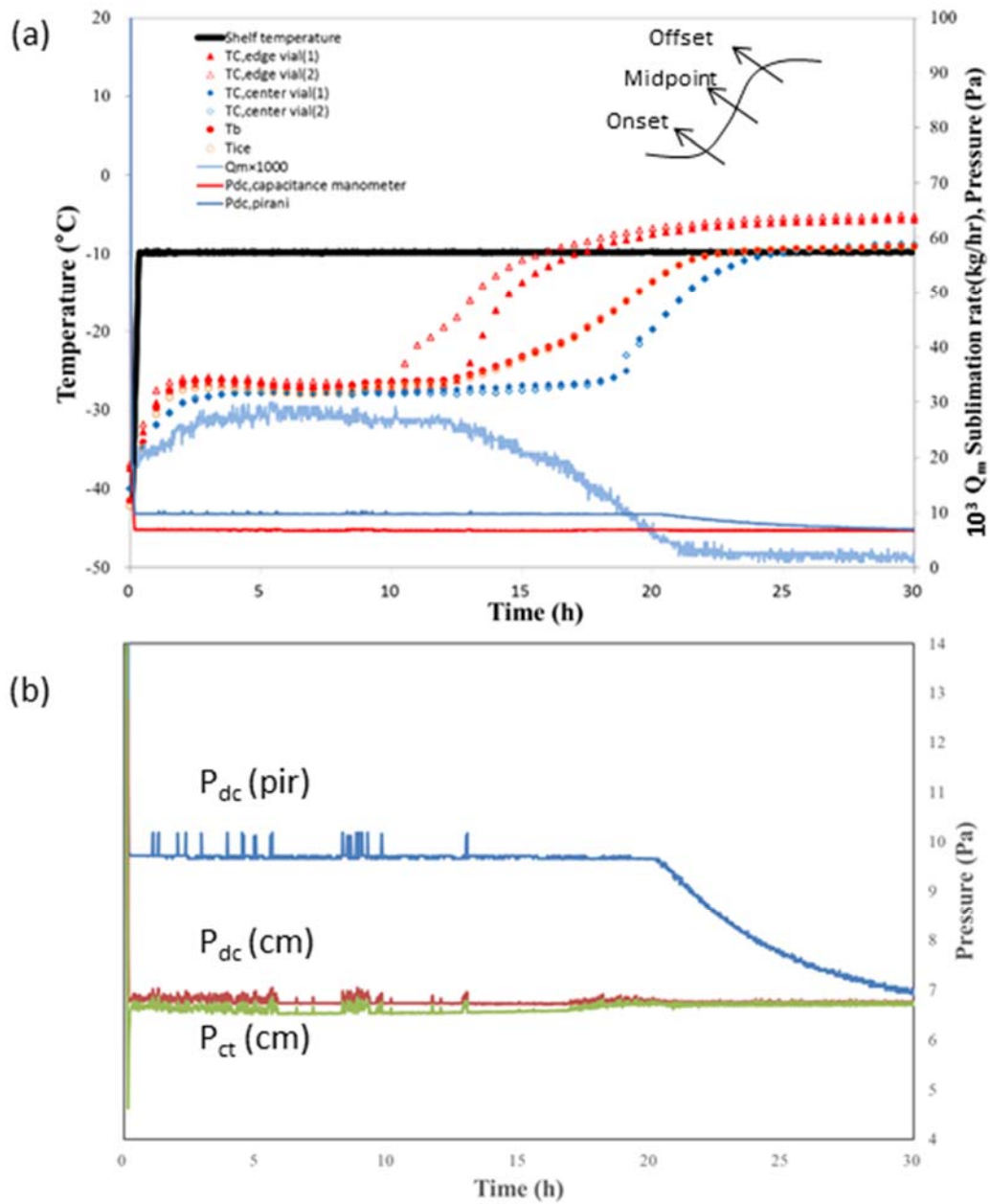


Figure 12 Temperature Profile during Primary Drying Monitored via TMbySR and TCs and Comparison of Primary Drying Endpoint Monitoring to Comparative Pressure.

Specifically, 220 vials filled with 3.15 mL of Flomoxef sodium bulk solution were lyophilized. Sublimation rate during primary drying was monitored via the TMbySR system. The determination of the end point for the primary drying stage (onset, midpoint, and offset) was based on previous studies [63].

Table 11 Comparison of Visual Inspections and Determination of the End Point of Primary Drying

Lot	Vial scale	Collapse of cake	PAT tool	Onset	Midpoint	Offset
01	220	No	TC*	18.5	20.5	24
			TMbySR	12.5	17.5	24
02	440	No	TC*	16.5	20	24
			TMbySR	12.5	17.5	24
03	660	No	TEMPRIS*	18.5	20.5	24
			TMbySR	12.5	17.5	24

* Information on the end point of the primary drying stage was read out from the temperature for the vial placed at the center.

4.3.2.2 440-Vial Scale

The above discussion is applicable for Lot 02 of the Flomoxef sodium bulk solution (440 vials scale) as shown in Figure 13(a), and the TMbySR system represented the same temperature profile of the batch and the same end point of the primary drying with Lot 01. Specifically, 440 lyophilized vials of Lot 02 were visually inspected and there was no cake collapse (Table 11). The measurement accuracy of the product temperature profile and ability to determine the end point of primary drying via the TMbySR system were confirmed as not dependent on the manufacturing scale. The Q_m value of Lot 02 obtained by TMbySR system was approximately 58×10^{-3} (kg/h) at the steady state ice sublimation, and the equivalent time of the product temperature profile calculated via the Q_m to the shelf temperature corresponded to 24 h (Figure 13(b)). Pirani pressure indicated the primary drying endpoint with a sharper pressure decrease towards the capacitance manometer pressure after 21 h. The TMbySR exhibited slightly better agreement with the primary drying endpoints as indicated by the TCs as opposed to comparative pressure. The temperature profile obtained by TMbySR system indicated that the representative temperature profile of the batch and end point of the primary

drying (as determined by TMbySR temperature reading) are in agreement with the end point detected via the TCs as shown in Table 3. Specifically, 440 lyophilized vials of Lot 02 were visually inspected and there was no cake collapse (Table 11).

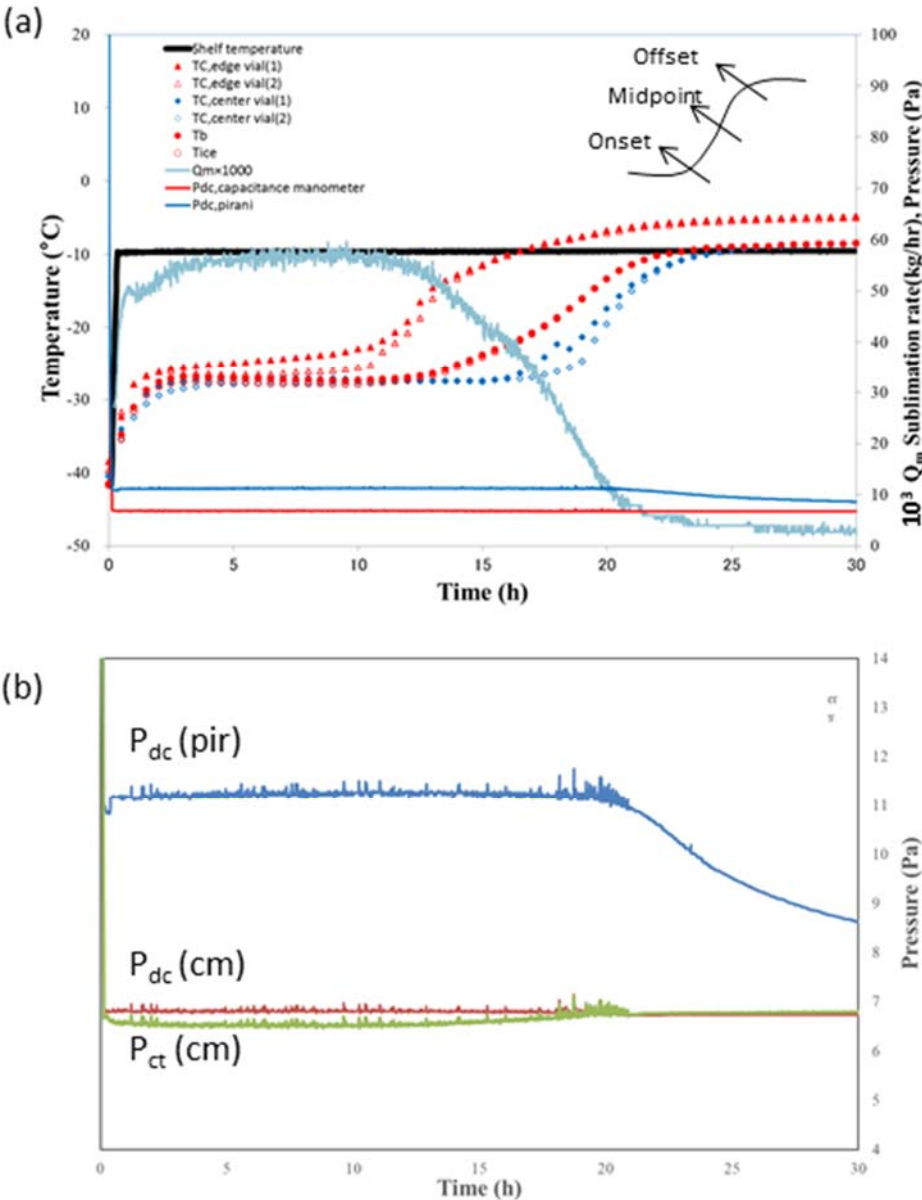


Figure 13 Temperature Profile during Primary Drying Monitored via TMbySR and TCs and Comparison of Primary Drying Endpoint Monitoring to Comparative Pressure.

Specifically, 440 vials filled with 3.15 mL of Flomoxef sodium bulk solution were lyophilized. The sublimation rate during primary drying was monitored via the TMbySR system. The determination of the end point for the primary drying stage (onset, midpoint, and offset) was based on previous studies [63].

4.3.3 Validation Study at 660-Vial Scale

In the last section, we tested the 220- and 440-vial scales to design the operation condition for 660-vial scale that corresponded to a maximum allowable scale in the present lyophilizer. The primary drying time was subsequently designed for 24 h based on the outcome of Lot 01 and 02 lyophilization with TMbySR system. It is difficult to adjust the TCs at the center bottom in the vials, and this causes variations in the T_b -profile of intra- and inter batch as shown in Figures 12(a) and 13(a). In the case of lyophilization at the 660-vial scale, we selected TEMPRIS as a reliable tool to measure the T_b -profile to compare it with TMbySR.

Figure 14(a) shows the result of temperature profile during the primary drying stage for the Flomoxef sodium bulk solution (Lot 3) monitored by TEMPRIS sensors and TMbySR system. Additionally, the sublimation rate Q_m data obtained by TMbySR system was recorded and compared to the comparative pressure. The TEMPRIS sensor was positioned at the bottom center in the vial and placed at the center position in the lyophilizer. It represented the longest steady state ice sublimation, and this was followed by a sharp increase step to the shelf temperature after 18.5 h and was essentially equilibrated to the T_s after 24 h. Additionally, TEMPRIS sensors positioned at the bottom center in the vials and placed at the edge position in the lyophilizer exhibited a shorter steady ice sublimation, and this was followed by a sharp increase step after 11 h. The T_b obtained by TMbySR system exhibited an intermediate temperature between the TEMPRIS sensors temperature placed at the center and edge position in the lyophilizer at the steady state ice sublimation, and this was followed by an increase step to T_s after 12.5 h and essentially equilibrated to T_s after 24 h. The essential equilibration time to

T_s obtained via the TMbySR temperature reading was in excellent agreement with the TEMPRIS sensor positioned at the bottom center in vials and placed at the center position in the lyophilizer. The sublimation rate Q_m of Lot 03 as obtained by TMbySR system was approximately 90×10^{-3} (kg/h) at steady state ice sublimation. After 12.5 h, the Q_m monotonously decreased until 21 h although a small peak of Q_m value was observed at approximately 26 h. It should be noted that the small Q_m -peak originated from the secondary drying process. Here, we discussed the behavior of Q_m value derived from the primary drying process. The equivalent time of the T_b -profile calculated via the Q_m to the T_s was 24 h. Pirani pressure indicated the primary drying endpoint with a sharper pressure decrease towards the capacitance manometer pressure after 21 h and the TMbySR exhibited a slightly better agreement with the primary drying endpoints indicated via the TEMPRIS sensors as opposed to the comparative pressure (also see Figure 14(b)).

After the completion of the lyophilization process, a visual inspection was conducted for all 660 vials. The results indicated *no cake collapse* and all lyophilized vials represented the *elegant cake appearance* as shown in Table 12. The water content of vials placed at the center and edge position in the lyophilizer is adequately controlled to the extent of 0.1% as shown in Table 12. Primary drying time designed by the TMbySR system was confirmed as appropriate from the quality assurance viewpoint for the drug product.

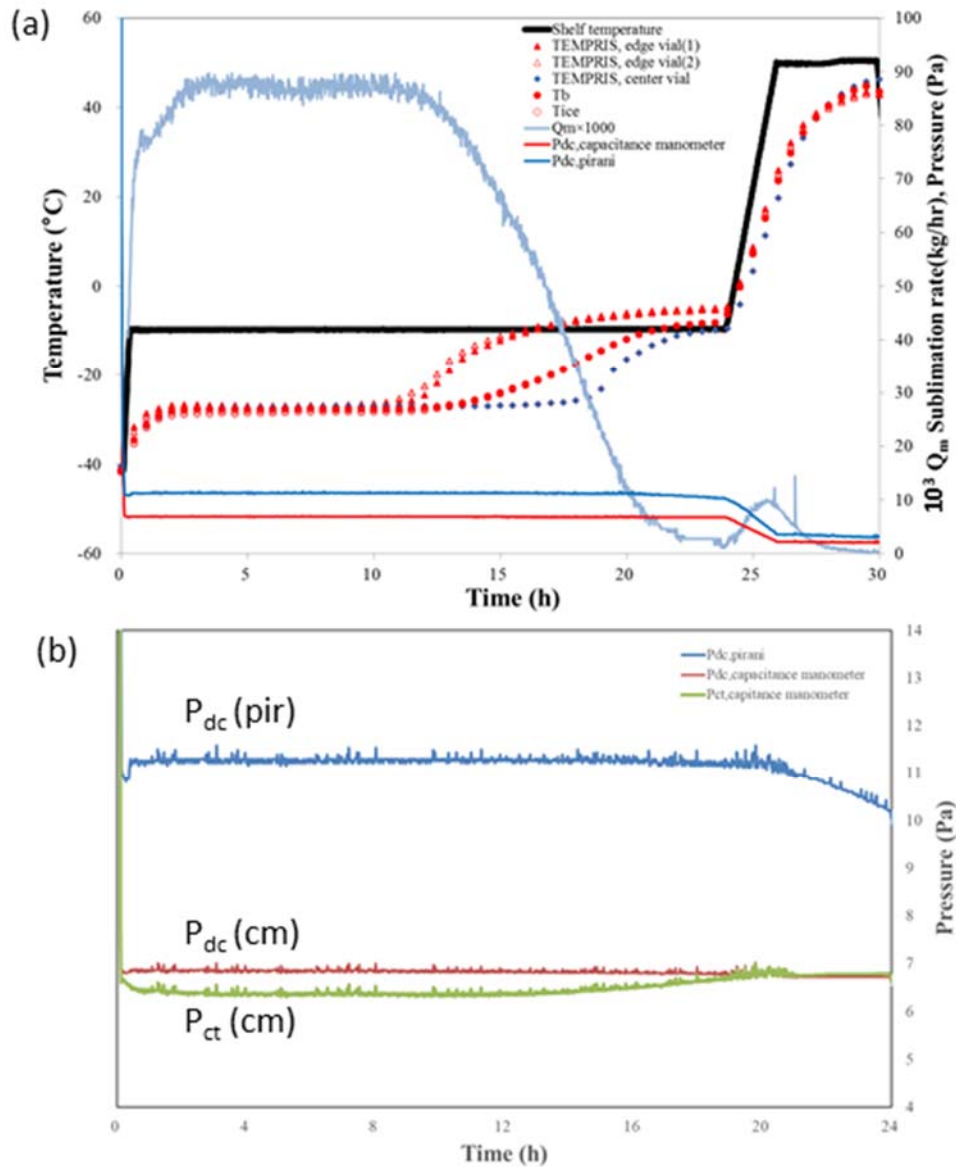
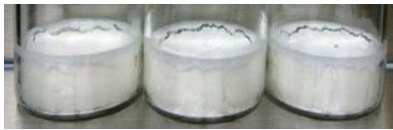





Figure 14 Temperature Profile during Primary Drying Monitored via TMbySR and TCs and Comparison of Primary Drying Endpoint Monitoring to Comparative Pressure.

Specifically, 660 vials filled with 3.15 mL of Flomoxef sodium bulk solution were lyophilized. Sublimation rate during primary drying was monitored via the TMbySR system. Determination of the end point for the primary drying stage (onset, midpoint, and offset) was based on previous studies [63].

Table 12 **Cake Appearance after Lyophilization**

		Cake Appearance		Water Content (%)*
Center Position	Front		Bottom	0.10 ± 0.01
	Bottom			
Edge Position	Front		Bottom	0.13 ± 0.02
	Bottom			

*Data were obtained from the triplicated experiments.

4.4 Conclusion

We developed a novel method to monitor the T_b value based on the sublimation rate of ice, and this was termed as TMbySR. The sublimation in vials caused the change in the chamber pressure P_{dc} and condenser pressure P_{ct} in the lyophilizer. Both P_{dc} and P_{ct} were measured via two capacitance manometers installed in the drying chamber and condenser of the lyophilizer, respectively. Hence, we estimated the C_r value to yield the experimental relationship corresponding to $C_r = 2.39 Q_m^{-1.09}$. The previous VMS did not consider the difference in the state of main pipe and valves for each lyophilizer, and thus we proposed that C_r should be clarified as a control constant via the water sublimation test. The result made it possible to monitor the Q_m value during primary drying. The minimum value of Q_m in the study corresponded to 0.0312 kg/h, and this was comparable to that reported for VMS [60]. The measurement of both the P_{dc} and P_{ct} values required the installation of high precision capacitance manometers based on the method since it was not necessary to equip an expensive

measuring instrument with the exception of a capacitance manometer, the Q_m value was easily monitored at low cost. The T_b -profile obtained by TMbySR represented the average T_b -profile of the batch. The end point of the primary drying as determined by the TMbySR system was in excellent agreement with the measurement via TC and TEMPRIS. Furthermore, data on the R_p value can be collected by measuring the T_{ice} and Q_m values. Thus, it is potentially possible to design an optimum drying program. The measurement accuracy of the T_b -profile and ability to determine the end point of primary drying by TMbySR system were confirmed in the manufacturing scale between 220 and 660 vials. The results of the study suggest that TMbySR system can be utilized for lyophilization cycle development, scale-up, and continuous cycle improvement via the seamless PAT strategy.

Chapter 5 General Conclusion

The objective of this thesis is to survey the promising strategy of lyophilization. In the thesis of chapter 1, scale-up procedure for primary drying process in lyophilizer by using the vial heat transfer and the drying resistance was investigated. In the thesis of chapter 2, the impact of ice nucleation technology on the quality and the productivity was researched. In the thesis of chapter 3, scalable PAT tool to be applied to commercial lyophilization process was developed. The outcomes of each chapter were summarized below.

Chapter 1

The objective of the study is to design primary drying conditions in a production lyophilizer based on a pilot lyophilizer. Although the shelf temperature and the chamber pressure need to be designed to maintain the sublimation interface temperature of the formulation below the collapse temperature, it is difficult to utilize a production lyophilizer to optimize cycle parameters for manufacturing. In this report, we assumed that the water vapor transfer resistance (R_p) in the pilot lyophilizer can be used in the commercial lyophilizer without any correction, under the condition where both lyophilizers were operated in the high efficiency particulate air (HEPA)-filtrated airflow condition. The shelf temperature and the drying time for the commercial manufacturing were designed based on the maximum R_p value calculated from the pilot lyophilizer (1,008 vials) under HEPA-filtrated airflow condition and from the vial heat transfer coefficient of the production lyophilizer (6,000 vials). And, the cycle parameters were verified using the production lyophilizer of 60,000 vials. It was therefore concluded that the operation of lab- or pilot-scale lyophilizer under HEPA-filtrated airflow condition was one of important factors for the scale-up.

Chapter 2

The freezing stage cannot be directly controlled, which leads to variation in product quality and low productivity during the lyophilization process. Our objective was to establish a robust design space for the primary drying stage using ice nucleation control based on the pressurization and depressurization technique. We evaluated the specific surface area (SSA), water content, scanning electron microscopy (SEM) images, and water vapor transfer resistance of the dried layer (R_p) of the products. The ice nucleation control resulted in a reduction of the SSA value and in an increase in water content. SEM observation suggested that the ice nucleation control enabled formation of large ice crystals, which was consistent with the reduction in the R_p value. As a result, the generation of collapsed cakes was inhibited, whereas 18% of the collapsed cakes were observed without ice nucleation control. Finally, this technique succeeded in determining a robust design space for the primary drying stage to produce uniform products of higher productivity. It was considered, from the present findings, that controlling the formation of large ice crystals impacted the product quality and productivity.

Chapter 3

Product temperature (T_b) and drying time constitute critical material attributes and process parameters in the lyophilization process and especially during the primary drying stage. In the study, we performed a temperature measurement by sublimation rate (TMbySR) to monitor the T_b value and determine the end point of primary drying. First, the water vapor transfer resistance coefficient through the main pipe from the chamber to the condenser (C_r) was

estimated by the water sublimation test. The use of C_r value made it possible to obtain the time course of T_b from the measurement of pressure at the drying chamber and at the condenser. Second, a Flomoxef sodium bulk solution was lyophilized by using the TMbySR system. The outcome was satisfactory when compared with that obtained via conventional sensors. The same was applicable for the determination of the end point of primary drying. A lab-scale application of the TMbySR system was evidenced via the experiment using 220-, 440-, and 660-vial scales of lyophilization. The outcome was not dependent on the loading amount. Thus, the results confirmed that the TMbySR system is a promising tool in laboratory scale.

Best practice for scale-up procedure and ice nucleation control is essential to establish robust design space for lyophilization process in commercial lyophilizer, and it is desirable to continuously monitor and analyze the designed lyophilization process by reliable and scalable PAT tool. We will continue to research and develop the lyophilization method using ice nucleation technology and seamless PAT tool in production scale. We believe our research contributes to robust designing of lyophilization process, shortening of the process development and stable supply of high-quality pharmaceutical drug products.

Further Perspectives

Several aspects to advance the technology in the pharmaceutical lyophilization are considered: new elemental technology, although conducted at small scale or attempted in the field other than the pharmaceutical field. For examples, a microwave-assisted freeze-drying (MFD) has been proposed in the food engineering field [64]. Freeze-drying coupled with a microwave heat source can speed up the drying rate and improve the product quality [64]. Few experiments are required to be extended from the laboratory scale to production one; the

knowledge or experiments are separated between different scales. With the goal to effectively scale-up the promising method at a lab-scale, the seamless scale-up procedure would be required.

The position-dependent model based on the thermodynamics for K_v has been improved previously [65]. As long as one of the operation conditions to achieve the same dynamic of R_p between pilot- and production scale lyophilizer, the methodology that the K_v value obtained at lab-scale is transferred to the production scale should be investigated to clarify the requisite condition for using the same K_v value after scale-up procedure. The further development of scale-up theory is expected to achieve the seamless use of K_v from the lab-scale for the production scale.

To reduce the cost impact at the primary drying stage can be in principle designed based on the equation (1) – (3).

$$K_v = \frac{\Delta H_s(dm/dt)}{A_v(T_s - T_b)} \quad 5 - (1)$$

$$K_v = a + \frac{bP_c}{1 + cP_c} \quad 5 - (2)$$

$$R_p = \frac{A_p(P_{ice} - P_c)}{(dm/dt)} \quad 5 - (3)$$

As evidently seen in these equations, the sublimation of ice is the important phenomena and its rate dm/dt is the most essential CPP in the primary drying stage. If not only K_v and R_p but

also T_b can be calculated from dm/dt at production scale, the operation system would be more robust. This motivation is identical to the VMS in PAT tool. At the present, an attempt using VMS has been limited to the lab-scale [66]. The possibility of scalable application of VMS would be required for the seamless use of K_v and R_p from the lab-scale; e.g. the influence of vial number on the shelves. As stated before, the ice nucleation control based on the freezing temperature makes it possible to control the dm/dt . Therefore, the application of the above technology would afford a seamless and rapid decision-making over the freezing and drying stages. This is one of the promising operation system for the lyophilization because the quality of products is no longer tested into them, *i.e.* quality –by-design.

In these years, a risk analysis for a pilot scale-freeze dryer has been reported for the construction of the basis for the risk-based decision-making in plant and process design of a freeze-dryer [67]. In the future, the PAT tool might contribute to the risk management of each scale-freeze dryer. Furthermore, the PAT tool would obtain the enormous big data from the equipment at each scale [68]. Important principle might be hidden behind the big data. For effective analysis, the use of the internet of things (IoT) together with big data from PAT tool and the models including CFD, would bring the rapid decision-making well fused with the practitioner's experiences [68-71]. We expect that the operational research based on IoT and big data will be developed.

Acknowledgement

I wish to express my sincere gratitude to Prof. Dr. Y. Kimura for providing me this precious study opportunity as a PhD student in his laboratory and for his steadfast support and encouragement. I always appreciate valuable feedbacks and suggestions offered by Dr. T. Shimanouchi. His inspiring thought and hospitality during my PhD work were unforgettable.

I gained a lot of technical and financial support from Shionogi & CO., LTD. I would like to thank my supervisor, Dr. G. Kimura and Mr. A. Mashimo for allowing me to conduct the research for the thesis. I learned the importance of obtaining PhD from Dr. G. Kimura and I got passion and courage from his great PhD thesis. Mr. A. Mashimo always managed my research progress and kindly supported me. I would like to thank Ms. K. Takahashi, Mr. M. Yamamoto, Mr. Y. Hamabe, and Mr. K. Honda. I got a lot of support to conduct the research from Shionogi colleagues.

Special thanks to Mr. H. Hosomi and Dr. H. Sawada, Kyowa Vacuum Engineering, CO., LTD. I had a lot of precious advice and useful information to apply TMbySR system to PAT tool in lyophilization.

Finally, I greatly thank my family, Yoshiko, Rio and Rimi, their dedicated support throughout my PhD work.

References

- [1] Nireesha GR., Divya L., Sowmya C., Venkateshan N., Niranjana Babu M., Lavakumar V., Lyophilization/Freeze Drying-An Review, *Int. J., Novel Trends Pharm. Sci.*, 3, 87-98 (2013).
- [2] Mahdavi S. A., Jafari S. M., Ghorbani M., Assadpoor E., Spray-drying microencapsulation of anthocyanins by natural biopolymers: A review, *Drying Tech.*, 32, 509-518 (2014).
- [3] Peighambaroust S.H., Golshan Tafti A., Hesari J., Application of spray drying for preservation of lactic acid starter cultures: a review, *Trends in Food Sci. Tech.*, 22, 215-224 (2011).
- [4] Freitas S., Merkle H. P., Gander B., Ultrasonic atomisation into reduced pressure atmosphere--envisaging aseptic spray-drying for microencapsulation, *J. Contr. Release*, 95, 185-195 (2004).
- [5] Matejtschuk P., Malik K., Duru C., *Ame. Pharm. Rev.*, 12, 54-58 (2009).
- [6] MJ Pikal, Freeze-drying of proteins. Part I: process design, *BioPharm.*, 3, 18-28 (1990)
- [7] JM Beals, MJ Edwards, MJ Pikal, JV Rinella, Jr., Formulations of obesity protein, Eur. Pat. Appl. (Eli Lilly and Co., USA). EP. 1997, pp.48
- [8] SL Nail and LA Gatin, Freeze-drying: principles and practice. In KE Avis, HA Lieberman, and L Lechman (eds.), *Pharmaceutical Dosage Forms: Parenteral Medications*, Vol. 2, MARCEL Dekker, New York, 1993, pp. 163-233
- [9] F Franks, Freeze drying: from empiricism to predictability. *Cryo-Letters*, 11, 93-110 (1990).
- [10] M. J. Pikal, S. Rambhatla, R. Ramot, The impact of the freezing stage in lyophilization: effects of the ice nucleation temperature on process design and product quality, *Am. Pharm. Rev.* 5, 48–53 (2002).
- [11] Tsinontides S. C., Rajniak P., Pham D., Hunke W. A., Placek J., Reynolds S. D., Freeze drying-principles and practice for successful scale-up to manufacturing, *J. Pharm.* 280, 1-16 (2004).
- [12] Kuu W. Y., Hardwick L. M., Akers M. J., Correlation of laboratory and production freeze drying cycles, *Int. J. Pharm.*, 302, 56-67 (2005).
- [13] Tang X. C., Pikal M. J., Design of freeze-drying processes for pharmaceuticals: practical advice, *Pharm. Res.*, 21, 191-200 (2004).
- [14] Department of Health and Human Services U.S Food and Drug Administration,

Pharmaceutical CGMPs for the 21st century - A risk based approach, 2002

- [15] Department of Health and Human Services U.S Food and Drug Administration, Guidance for industry: PAT - A frame-work for innovative pharmaceutical development, manufacturing and quality assurance, 2004
- [16] International conference on harmonization of technical requirements for registration of pharmaceuticals for human use. ICH Harmonized Tripartite Guidance. Pharmaceutical Developent Q8 (R2), August 2009.
- [17] Nail SL, Searles JA, Elements of quality by design in development and scale-up of freeze-dried parenterals, *Int. BioPharm.*, 21, 44-52 (2008).
- [18] Department of Health and Human Services U.S Food and Drug Administration, How to identify critical quality attributes and critical process parameters, FDA/PQRI 2nd Conference North Bethesda, Maryland Oct. 2015
- [19] Robert A. L, Sau LL, Lai ML, Andre R, Lawrence X. Y, Quality by Design: Concepts for ANDAs, *AAPS J.* 10 (2), 268-276 (2008)
- [20] Franks F., *Eur. J. Pharm. Biopharm.*, **45**, 221–229 (1998).
- [21] Liu J., Viverette T., Virgin M., Anderson M., Dalal P., *Pharm. Dev. Technol.*, **10**, 261–272 (2005).
- [22] Pikal M. J., Rambhatla S., Ramot R., *Am. Pharm. Rev.*, **5**, 48–53 (2002).
- [23] Fissore D., Barresi A. A., *Drying Tech.*, **29**, 1673–1684 (2011).
- [24] Pisano R., Fissore D., Barresi A. A., Rastelli M., *AAPS PharmSciTech*, **14**, 1137–1149 (2013).
- [25] Kodama T., Sawada H., Hosomi H., Takeuchi M., Wakiyama N., Yonemochi E., Terada K., *Chem. Pharm. Bull.*, **62**, 153–159 (2014).
- [26] Pikal M. J., *J. Parenter. Sci. Technol.*, **39**, 115–139 (1985).
- [27] Patapoff T. W., Overcashier D. E., *Biopharm.*, **15**, 16–21 (2002).
- [28] Nail S. L., Jiaang S., Chongprasert S., Knopp S. A., “Fundamentals of freeze-drying,” ed. by Nail. S. L., Akers M. J., Kluwer Academic/Plenum Publisher, New York, 2002.
- [29] Pikal M. J., Shah S., *Int. J. Pharm.*, 62, 165–186 (1990).
- [30] Pikal M. J., Bogner R., Mudhivarthi V., Sharma P., Sane P., *J. Pharm. Sci.*, **105**, 3333–3343 (2016).
- [31] Rambhatla S., Pikal M. J., *AAPS PharmSciTech*, **4**, 22–31 (2003).
- [32] Gan K. H., Bruttini R., Crosser O. K., Liapis A. I., *Int. J. Heat Mass Transfer*, **48**, 1675–1687 (2005).
- [33] Pikal M. J., Roy M. L., Shah S., *J. Pharm. Sci.*, 73, 1224–1237 (1984).

- [34] Patel S. M., Pikal M. J. *J. Pharm. Sci., Commentary*, **1–5** (2013). 10.1002/jps23703
- [35] Rambhatla S., Pikal M. J., “Heat and mass transfer issues in freeze- drying process development,” ed. by Constantino H. R., AAPS Press, Arlington, VA, U.S.A., 2004.
- [36] Nail S. L., *J. Parenter. Drug Assoc.*, **34**, 358–368 (1980).
- [37] Tang X. C., Nail S. L., Pikal M. J., *AAPS PharmSciTech*, **7**, E105– E111 (2006).
- [38] Tang X. C., Nail S. L., Pikal M. J., *Pharm. Res.*, **22**, 685–700 (2005).
- [39] Moore E. B., Molinero V., *Nature* (London), **479**, 506–508 (2011).
- [40] Searles J. A., Carpenter J. F., Randolph T. W., *J. Pharm. Sci.*, **90**,860–871 (2001).
- [41] Roy M. L., Pikal M. J., *PDA J. Pharm. Sci. Technol.*, **43**, 60–66 (1989).
- [42] Pikal M. J., Shah S., Roy M. L., Putman R., *Int. J. Pharm.*, **60**,203–207 (1990).
- [43] Geidobler R., Winter G., *Eur. J. Pharm. Biopharm.*, **85**, 214–222 (2013).
- [44] Kasper J. C., Friess W., *Eur. J. Pharm. Biopharm.*, **78**, 248–263 (2011).
- [45] Konstantinidis A. K., Kuu W., Otten L., Nail S. L., Sever R. R., J.
- [46] Gasteyer T. H., Sever R. R., Hunek B., Grinter N., Verdone M. L., Patent US20070186437 (2007).
- [47] Pisano R., Fissore D., Barresi A. A., Brayard P., Chouvenc P., Woi- net B., *Pharm. Dev. Technol.*, **18**, 280–295 (2013).
- [48] Rambhatla S., Pikal M. J., *AAPS PharmSciTech*, **4**, 22–31 (2003)
- [49] Tang X. C., Nail S. L., Pikal M. J., *AAPS PharmSciTech*, **7**, E77–E84 (2006).
- [50] H. Kawasaki, T. Shimanouchi, M. Yamamoto, K. Takahashi, Y. Kimura, Scale-up procedure for primary drying process in lyophilizer by using the vial heat transfer and the drying resistance, *Chem. Pharm. Bulletin.*, **66** (11), 1048-1056 (2018)
- [51] H. Kawasaki, T. Shimanouchi, K. Takahashi, Y. Kimura, Effect of controlled nucleation of ice crystals on the primary drying stage during lyophilization, *Chem. Pharm. Bulletin.*, **66** (12), 1-10 (2018)
- [52] Patel SM, Pikal MJ. 2009. Process analytical technologies (PAT) in freeze-drying of parenteral products. *Pharm Dev Technol* **14**(6): 567–587.
- [53] Oetjen GW, Haseley P. 2004. *Freeze-Drying*, Wiley-VCH, Weinheim, Germany
- [54] Schneid S, Gieseler H. 2008. Evaluation of a New Wireless Temperature Remote Interrogation System (TEMPRIS) to Measure Product Temperature During Freeze Drying, *AAPS Pharm Sci Tech* **9** (3): 729-739.
- [55] Nail SL, Johnson W. 1992. Methodology for in-process determination of residual water in freeze-dried products. *Dev Biol Stand.* **74**: 137–51.

- [56] Patel SM, Doen T, Pikal MJ. 2009. Determination of end point of primary drying in freeze-drying process control. *AAPS Pharm Sci Tech* 11 (1): 73-84.
- [57] Connelly JP, Welch JV. 1993. Monitor lyophilization with mass spectrometer gas analysis. *PDA J Pharm Sci Tech* 47:70–5.
- [58] Gieseler H, Kessler WJ, Finson M, Davis SJ, Mulhall PA, Bons V. 2007. Evaluation of tunable diode laser absorption spectroscopy for in-process water vapor mass flux measurements during freeze drying. *J Pharm Sci* 96 (7): 1776–93.
- [59] Schneid SC, Gieseler H, Kessler WJ, Pikal MJ. 2009. Non-invasive product temperature determination during primary drying using tunable diode laser absorption spectroscopy. *J. Pharm. Sci* 98: 3406-3418.
- [60] Pisano R, Fissore D, Barresi AA. 2016. Noninvasive monitoring of a freeze-drying process for *tert*-butanol/water cosolvent-based formulations. *Ind Eng Chem Res* 55: 5670-5680.
- [61] Fissore D. 2017. Model-based PAT for quality management in pharmaceuticals freeze-drying: state of the art. *Vrontiers in Bioeng Biotechnol* 5 (doi: 10.3389/fbioe.2017.00005)
- [62] Sawada H, Tonegawa K, Hosomi H, Sunama R. 2016. Calculation method and calculation device for sublimation interface temperature, bottom part temperature, and sublimation rate of material to be dried in freeze-drying device. US9488410B2.
- [63] Khairnar S, Kini R, Harwalkar M, Salunkhe K, Chaudhari SR. 2013. A Review on Freeze Drying Process of Pharmaceuticals. *Int. J. Res. Pharm* 4: 76-94.
- [64] K. Fan, M. Zhang, A.S. Mujumdar, Recent developments in high efficient freeze-drying of fruits and vegetables assisted by microwave: A review, *Critical Reviews in Food Science and Nutrition*, 2018 (<https://doi.org/10.1080/10408398.2017.1420624>) (accessed November 2018)
- [65] Pikal M. J., Bogner R., Mudhivartha V., Sharma P., Sane P., Freeze-Drying Process Development and Scale-Up: Scale-Up of Edge Vial Versus Center Vial Heat Transfer Coefficients, *K_v, J. Pharm. Sci.*, 105, 3333-3343 (2016).
- [66] D. Fissore, Model-based PAT for quality management in pharmaceuticals freeze-drying: state of the art, *Vrontiers in Bioeng. Biotechnol.*, 5 (2017) (doi: 10.3389/fbioe.2017.00005)

- [67] S. Bosca, D. Fissore, M. Demichela, Reliability Assessment in a Freeze-Drying Process, *Ind. Eng. Chem. Res.*, 56, 6685-6694 (2017)
- [68] Dossetter AG, Ecker G, Laverty H, Overington J., 'Big data' in pharmaceutical science: challenges and opportunities, *Future Med Chem.* 6(8),857-64(2014)
- [69] Richter L, Ecker GF., Medicinal chemistry in the era of big data, *Drug Discov Today Technol.* 14,37-41(2015)
- [70] Lusher SJ, McGuire R, van Schaik RC, Nicholson CD, de Vlieg J., Data-driven medicinal chemistry in the era of big data, *Drug Discov Today.* 19(7),859-68(2014)
- [71] Lusher SJ, Ritschel T., Finding the right approach to big data-driven medicinal chemistry, *Future Med Chem.* 7(10),1213-6 (2015)

Refereed Papers

1. H. Kawasaki, T. Shimanouchi, M. Yamamoto, K. Takahashi, Y. Kimura, Scale-up procedure for primary drying process in lyophilizer by using the vial heat transfer and the drying resistance, *Chem. Pharm. Bulletin.*, 66 (11), 1048-1056 (2018)
2. H. Kawasaki, T. Shimanouchi, K. Takahashi, Y. Kimura, Effect of controlled nucleation of ice crystals on the primary drying stage during lyophilization, *Chem. Pharm. Bulletin.*, 66 (12), 1-10 (2018)
3. H. Kawasaki, T. Shimanouchi, H. Sawada, H. Hosomi, Y. Hamabe, Y. Kimura, Temperature Measurement by Sublimation Rate as a Process Analytical Technology Tool in Lyophilization, *J. Pharm. Sci* (Submitted).
4. H. Kawasaki, T. Shimanouchi, Y. Kimura, Sublimation and development of scale-up recipe, controlled ice nucleation, and process analytical technology., *J. Chem* (Submitted).